Massachusetts Institute of Technology

Search for a Higgs boson in the mass range from 145 to 1000 GeV decaying to a pair of W or Z bosons

The CMS collaboration

E-mail: cms-publication-committee-chair@cern.ch

ABSTRACT: A search for a heavy Higgs boson in the H → WW and H → ZZ decay channels is reported. The search is based upon proton-proton collision data samples corresponding to an integrated luminosity of up to $5.1\,\text{fb}^{-1}$ at $\sqrt{s} = 7\,\text{TeV}$ and up to 19.7fb^{-1} at $\sqrt{s} = 8\,\text{TeV}$, recorded by the CMS experiment at the CERN LHC. Several final states of the H → WW and H → ZZ decays are analyzed. The combined upper limit at the 95% confidence level on the product of the cross section and branching fraction exclude a Higgs boson with standard model-like couplings and decays in the range $145 < m_\text{H} < 1000\,\text{GeV}$. We also interpret the results in the context of an electroweak singlet extension of the standard model.

Contents

1 Introduction

The standard model (SM) of electroweak (EW) interactions [1–3] posits the existence of the Higgs boson, a scalar particle associated with the field responsible for spontaneous EW symmetry breaking [4–9]. The mass of the boson is not predicted by the theory. In 2012 the ATLAS and CMS collaborations at the CERN LHC reported the observation of a new boson with a mass of about 125 GeV [10–14]. Throughout this paper, we denote the observed Higgs boson as h(125). Subsequent studies of the production and decay rates [15–25] and of the spin-parity quantum numbers [18, 19, 26, 27] of the new boson show that its properties are compatible with those expected for the SM Higgs boson.

The observation of a Higgs boson with a mass of 125 GeV is also consistent with the unitarity constraints on diboson scattering at high energies [28–37]. Nevertheless, there is a possibility that the newly discovered particle is part of a larger Higgs boson sector and

thus only partially responsible for EW symmetry breaking. This can be realized in several scenarios, such as two-Higgs-doublet models [38, 39], or models in which the SM Higgs boson mixes with a heavy EW singlet [40–63], which predict the existence of additional resonances at high mass, with couplings similar to those of the SM Higgs boson.

Previous searches at the LHC for heavy SM-like Higgs bosons have been reported by ATLAS and CMS. Based on a dataset of $4.7\,\text{fb}^{-1}$ at $\sqrt{s} = 7\,\text{TeV}$ and up to $5.9\,\text{fb}^{-1}$ at $\sqrt{s} = 8\,\text{TeV}$, and combining all channels listed in ref. [10], ATLAS excludes a SM-like heavy Higgs boson of $131 < m_\text{H} < 559\,\text{GeV}$ at 95% CL [10]. The CMS collaboration reported a search in the WW and ZZ decay channels using an initial dataset of $5.1\,\text{fb}^{-1}$ at $\sqrt{s} = 7\,\text{TeV}$ and $5.3\,\text{fb}^{-1}$ at $\sqrt{s} = 8\,\text{TeV}$, searching in the mass range $145 < m_\text{H} < 1000\,\text{GeV}$, and excluding Higgs boson masses up to $710\,\text{GeV}$ at 95% CL [64]. In this paper, we report on an extension of this search using the complete 7 and 8 TeV dataset. In addition, the search is interpreted in the context of the SM expanded by an additional EW singlet. Both the SM-like heavy Higgs boson as well as the EW singlet are denoted as H here.

The analysis uses proton-proton collision data recorded with the CMS detector, corresponding to integrated luminosities of up to $5.1\,\text{fb}^{-1}$ at $\sqrt{s} = 7\,\text{TeV}$ and up to $19.7\,\text{fb}^{-1}$ at $\sqrt{s} = 8\,\text{TeV}$. The analysis is performed in a mass range $145 < m_\text{H} < 1000\,\text{GeV}$ exploiting both the H $\rightarrow$ WW and H $\rightarrow$ ZZ decay channels, with the lower boundary being chosen to reduce contamination from h(125). In the case of a Higgs boson decaying into a pair of W bosons, the fully leptonic (H $\rightarrow$ WW $\rightarrow \ell\nu\ell\nu$) and semileptonic (H $\rightarrow$ WW $\rightarrow \ell\nu$qq) final states are considered in the analysis. For a Higgs boson decaying into two Z bosons, final states containing four charged leptons (H $\rightarrow$ ZZ $\rightarrow 2\ell2\ell'$), two charged leptons and two quarks (H $\rightarrow$ ZZ $\rightarrow 2\ell2$q), and two charged leptons and two neutrinos (H $\rightarrow$ ZZ $\rightarrow 2\ell2\nu$) are considered, where $\ell = $ e or μ and $\ell' = $ e, μ, or τ.

2   CMS detector

The central feature of the CMS apparatus is a superconducting solenoid of 6 m internal diameter, providing a magnetic field of 3.8 T. Within the solenoid volume are a silicon pixel and strip tracker, a lead tungstate crystal electromagnetic calorimeter (ECAL), and a brass and scintillator hadron calorimeter, each composed of a barrel and two endcap sections. Muons are measured in gas-ionization detectors embedded in the steel flux-return yoke outside the solenoid. Extensive forward calorimetry complements the coverage provided by the barrel and endcap detectors. The first level of the CMS trigger system, composed of custom hardware processors, uses information from the calorimeters and the muon detectors to select the most interesting events in a fixed time interval of less than $4\,\mu$s. The high level trigger processor farm further decreases the event rate from around 100 kHz to less than 1 kHz, before data storage. A more detailed description of the detector as well as the definition of the coordinate system and relevant kinematic variables can be found in ref. [65].

3   Signal model and simulations

Several Monte Carlo event generators are used to simulate the signal and background event samples. The Higgs boson signal samples from gluon fusion (ggF, gg $\rightarrow$ H), and vector

boson fusion (VBF, qq → qqH), are generated with POWHEG 1.0 [66–70] at next-to-leading order (NLO) and a dedicated program [71] used for angular correlations. Samples of WH, ZH, and t̄tH events are generated using the leading-order (LO) PYTHIA 6.4 [72] program. At the generator level, events are weighted according to the total cross section $\sigma(\text{pp} \to \text{H})$ [73], which contains contributions from ggF computed to next-to-next-to-leading order (NNLO) and next-to-next-to-leading-log (NNLL), and from weak-boson fusion computed at NNLO. The WW(ZZ) invariant mass, m_{WW} (m_{ZZ}), lineshape is affected by interference between signal and SM background processes. The simulated m_{H} lineshape is therefore corrected to match theoretical predictions [74–76] using the complex-pole scheme for the Higgs boson propagator. The procedure for including lineshape corrections and uncertainties from interference of the signal with background processes for both ggF and VBF production are described below in the discussion of the lineshape corrections applied for the EW singlet interpretation.

The background contribution from q̄q → WW production is generated using MAD-GRAPH 5.1 [77], and the subdominant gg → WW process is generated at LO with GG2WW 3.1 [78]. The q̄q → ZZ production process is simulated at NLO with POWHEG, and the gg → ZZ process is simulated at LO using GG2ZZ 3.1 [79]. Other diboson processes (WZ, $Z\gamma^{(*)}$, $W\gamma^{(*)}$), Z+jets, and W+jets are generated with PYTHIA and MADGRAPH. The t̄t and tW events are generated at NLO with POWHEG. For all samples, PYTHIA is used for parton showering, hadronization, and underlying event simulation. For LO generators, the default set of parton distribution functions (PDF) used to produce these samples is CTEQ6L [80], while CT10 [81] is used for NLO generators. The tau lepton decays are simulated with TAUOLA [82]. The detector response is simulated using a detailed description of the CMS detector, based on the GEANT4 package [83], with event reconstruction performed identically to that of recorded data. The simulated samples include the effect of multiple pp interactions per bunch crossing (pileup). The PYTHIA parameters for the underlying events and pileup interactions are set to the Z2 (Z2*) tune [84] for the 7 (8) TeV simulated data sample, with the pileup multiplicity distribution matching the one observed in data.

The data are analysed to search for both a beyond the standard model (BSM) case in the form of an EW singlet scalar mixed with the recently discovered Higgs boson, h(125), as well as a heavy Higgs boson with SM-like couplings. The couplings of the two gauge eigenstates (h(125) and EW singlet) are phenomenologically constrained by unitarity and the coupling strength of the light Higgs boson is therefore reduced with respect to the SM case. The unitarity constraint is ensured by enforcing $C^2 + C'^2 = 1$, where C and C' are defined as the scale factors of the couplings with respect to the SM of the low- and high-mass Higgs boson, respectively. The EW singlet production cross section is also modified by a factor μ' and the modified width is Γ'; they are defined as

$$\mu' = C'^2 \left(1 - \mathcal{B}_{\text{new}}\right), \tag{3.1}$$

$$\Gamma' = \Gamma_{\text{SM}} \frac{C'^2}{1 - \mathcal{B}_{\text{new}}}, \tag{3.2}$$

where $\mathcal{B}_{\text{new}}$ is the branching fraction of the EW singlet to non-SM decay modes. An upper

limit at 95% CL can be set indirectly as $C'^2 < 0.28$ using the signal strength fits to the h(125) boson as obtained in ref. [85].

This paper focuses on the case where $C'^2 \leq (1 - \mathcal{B}_{\text{new}})$. In this regime the new state is expected to have an equal or narrower width with respect to the SM case. Results are presented distinguishing between the $\mathcal{B}_{\text{new}} = 0$ and $\mathcal{B}_{\text{new}} > 0$ cases. Under this hypothesis, signal samples with different Higgs boson widths are generated, scanning the C'^2 and $\mathcal{B}_{\text{new}}$ space. We follow the recommendations of the "LHC Higgs Cross section Working Group" [73] described below.

The SM signal mass lineshape generated with POWHEG is weighted in order to simulate the narrow scalar singlet lineshape. For the ggF production mode, the weights are calculated using either the GG2ZZ generator for the ZZ channel, or the POWHEG and MCFM 6.2 [86] generators for the interference calculation for the WW channel. For the VBF production mode, the interference weights are computed using the PHANTOM 1.2 [87] generator, where the signal-only lineshape at LO is weighted based on results obtained with MADGRAPH generator predictions. The weights are defined as the ratio of the sum of a narrow resonance signal plus interference and the standard model signal lineshape as generated. The contribution from the interference term between the BSM Higgs boson and the background is furthermore assumed to scale according to the modified coupling of the Higgs boson as $(\mu + I)_{\text{BSM}} = \mu_{\text{SM}} C'^2 + I_{\text{SM}} C'$, where $\mu(I)$ is the signal strength (interference) in the BSM or SM cases. This assumption is based on the hypothesis that the couplings are similar to the SM case and simply rescale due to unitarity constraints. Systematic uncertainties considered for this procedure are detailed later.

If the new resonance has a very small width, its production will tend to interfere less with the background continuum. Thus in the most interesting region of low-C'^2, the effect of the interference and its exact modeling is of limited importance. Any possible interference between h(125) and its EW singlet partner [88, 89] is assumed to be covered by a conservative systematic uncertainty. In addition to the EW singlet, the analysis searches for a heavy Higgs boson that gets produced and decays like the SM Higgs boson, but has a higher mass and interferes with h(125).

4 Event reconstruction

CMS uses a particle-flow (PF) reconstruction algorithm [90, 91] to provide an event description in the form of particle candidates, which are then used to build higher-level objects, such as jets and missing transverse energy, as well as lepton isolation quantities. Not all the channels considered here use the same selection criteria for their objects, but the common reconstruction methods are listed below.

The high instantaneous luminosity delivered by the LHC provides an average of about 9 (21) pileup interactions per bunch crossing in 7 (8) TeV data, leading to events with several possible primary vertices. The vertex with largest value of the sum of the square of the transverse momenta (p_{T}) for the associated tracks is chosen to be the reference vertex. According to simulation, this requirement provides the correct primary vertex in more than 99% of both signal and background events.

Muon candidates are reconstructed by using one of two algorithms: one in which tracks in the silicon tracker are matched to hits in the muon detectors, and another in which a combined fit is performed to signals in both the silicon tracker and the muon system. Other identification criteria based on the number of measurements in the tracker and in the muon system, the fit quality of the muon track, and its consistency with its origin from the primary vertex are also imposed on the muon candidates to reduce the misidentification rate [92]. In some of the channels, vetos are imposed on additional low-p_T muons in the event, whose tracks in the silicon tracker fulfill more stringent requirements, but whose primary vertex association can be more relaxed. We call these muons *soft* muons.

Electron candidates are reconstructed from superclusters, which are arrays of energy clusters along the ϕ direction in the ECAL, matched to tracks in the silicon tracker. A complementary algorithm reconstructs electron candidates by extrapolating measurements in the innermost tracker layers outward to the ECAL. Trajectories from both algorithms are reconstructed using the Gaussian sum filter algorithm [93], which accounts for the electron energy loss by bremsstrahlung. Additional requirements are applied to reject electrons originating from photon conversions in the tracker material. Electron identification relies on a multivariate discriminant that combines observables sensitive to the bremsstrahlung along the electron trajectory, the geometrical and momentum-energy matching between the electron trajectory and the associated supercluster, as well as ECAL shower shape observables. Electron candidates with a pseudorapidity η of their ECAL supercluster in the transition region between ECAL barrel and endcap ($1.4442 < |\eta| < 1.5660$) are rejected, because the reconstruction of electrons in this region is compromised [94].

The PF candidates are used to reconstruct hadronic tau candidates, τ_h, with the "hadron plus strip" algorithm [95] that is designed to optimize the performance of τ_h identification and reconstruction by considering specific τ_h decay modes. The neutrinos produced in all τ decays escape detection and are ignored in the τ_h reconstruction. The algorithm provides high τ_h identification efficiency, approximately 50% for the range of τ_h energies relevant for this analysis, while keeping the misidentification rate for jets at the level of $\sim 1\%$.

Leptons produced in the decay of W and Z bosons are expected to be isolated from hadronic activity in the event. Isolation is defined as the scalar sum of the transverse momenta of the PF candidates found (excluding the selected leptons in the event themselves) in a cone of radius $R = \sqrt{\Delta\eta^2 + \Delta\phi^2} = 0.4$, with ϕ being measured in radians, built around each lepton. We require that the isolation sum is smaller than 20% (15%) of the muon (electron) transverse momentum. To account for the contribution to the isolation sum from pileup interactions and the underlying event, a median energy density is determined on an event-by-event basis using the method described in ref. [96]. For electron candidates, an effective area that is proportional to the isolation cone, is derived to renormalize this density estimate to the number of pileup interactions, and is subtracted from the isolation sum. For muon and tau candidates, the correction is done by subtracting half the sum of the transverse momenta of the charged particles not associated to the primary vertex in the cone of interest. Soft muons do not need to fulfill isolation requirements.

The combined efficiency of lepton reconstruction, identification, and isolation is measured using observed Z decays and ranges between 90% and 97% for muons, between 70% and 90% for electrons, and approximately 50% for hadronic taus depending on the p_T and η of the leptons.

Jets are reconstructed from PF candidates [97] using the anti-k_T clustering algorithm [98] with a distance parameter of 0.5 (called AK5 jets), as implemented in the FASTJET package [99], and with the Cambridge-Aachen algorithm [100] with a distance parameter of 0.8 (called CA8 jets); when not otherwise specified we use the term *jets* to mean AK5 jets throughout this paper. Any reconstructed jet overlapping with isolated leptons within a distance of 0.5 (0.8) for AK5 (CA8) jets is removed in order to avoid double counting the lepton as a jet. AK5 (CA8) jets are required to have $|\eta| < 4.7\,(2.4)$. At hadron level, the jet momentum is defined as the vectorial sum of all particle momenta in the jet, and is found in the simulation to be within 5–10% of the true momentum over the whole p_T range and detector acceptance. A correction is applied to the jet p_T to take into account the extra energy clustered in jets due to additional proton-proton interactions within the same bunch crossing [96, 101]. Other jet energy scale (JES) corrections applied are derived from the simulation, and are calibrated with in situ measurements of the energy balance of dijet and Z/γ+jets events. For some of the channels in this analysis, a combinatorial background arises from low-p_T jets from pileup interactions, which get clustered into high-p_T jets. At $\sqrt{s} = 8$ TeV the number of pileup events is larger than at $\sqrt{s} = 7$ TeV, and a multivariate selection is applied to separate jets stemming from the primary interaction and those reconstructed due to energy deposits associated with pileup interactions [102]. The discrimination is based on the differences in the jet shapes, on the relative multiplicity of charged and neutral components, and on the different fraction of transverse momentum, which is carried by the hardest components. Within the tracker acceptance, the tracks belonging to each jet are also required to be compatible with the primary vertex.

At high Higgs boson masses, the p_T of the Z or W boson is high enough that the two quarks from the vector boson decay are expected to be reconstructed as a single CA8 jet, or *merged* jet. To improve background rejection and jet mass resolution, we apply a jet pruning algorithm [103]. Additionally, the "N-subjettiness ratio" variable τ_2/τ_1, a measure of the compatibility of a jet having $N = 2$ subjets, is used to reduce the backgrounds [103, 104]. We require $\tau_2/\tau_1 < 0.5$ to avoid contamination from jets originating from the hadronization of gluons and single quarks.

In some of the channels included in this analysis, the identification of jets originating from b quarks is important. These b jets are tagged with dedicated algorithms [105], which are applied either directly to the AK5 jets, or to the subjets of the merged jets. The b-tagging algorithm used is either the Combined Secondary Vertex algorithm, Jet Probability algorithm, or Track Counting High Efficiency algorithm depending on the channel. Tagged b-jet candidates are required to have $p_T > 30$ GeV and to be within the tracker acceptance ($|\eta| < 2.4$). For jets in this kinematic range with a b-tagging efficiency of 70%, the misidentification probability from light quark and gluon jets is approximately 1%.

The missing transverse momentum vector, $\vec{E}_T^{\text{miss}}$, is defined as the projection on the plane perpendicular to the beams of the negative vector sum of the momenta of all reconstructed particles in an event [91, 106]. Its magnitude is referred to as E_T^{miss}.

H decay mode	H production	Exclusive final states	No. of channels	m_H range [GeV]	m_H resolution
$WW \to \ell\nu\ell\nu$	untagged	$((ee, \mu\mu), e\mu) + (0 \text{ or } 1 \text{ jets})$	4	145–1000[ab]	20%
	VBF tag	$((ee, \mu\mu), e\mu) + (jj)_{VBF}$	2	145–1000 [ab]	20%
$WW \to \ell\nu qq$	untagged	$(e\nu, \mu\nu) + (jj)_W$	2	180–600	5–15%
	untagged	$(e\nu, \mu\nu) + (J)_W + (0+1\text{-jets})$	2	600–1000 [b]	5–15%
	VBF tag	$(e\nu, \mu\nu) + (J)_W + (jj)_{VBF}$	1	600–1000 [b]	5–15%
$ZZ \to 2\ell2\ell'$	untagged	$4e, 4\mu, 2e2\mu$	3	145–1000	1–2%
	VBF tag	$(4e, 4\mu, 2e2\mu) + (jj)_{VBF}$	3	145–1000	1–2%
	untagged	$(ee, \mu\mu) + (\tau_h\tau_h, \tau_e\tau_h, \tau_\mu\tau_h, \tau_e\tau_\mu)$	8	200–1000	10–15%
$ZZ \to 2\ell2\nu$	untagged	$(ee, \mu\mu) + (0 \text{ or } \geq 1 \text{ jets})$	4	200–1000	7%
	VBF tag	$(ee, \mu\mu) + (jj)_{VBF}$	2	200–1000	7%
$ZZ \to 2\ell2q$	untagged	$(ee, \mu\mu) + (jj)_Z^{0,1,2\,b\,tags}$	6	230–1000[c]	3%
	untagged	$(ee, \mu\mu) + (J)_Z^{0,1,2\,b\,tags}$	6	230–1000 [c]	3%
	VBF tag	$(ee, \mu\mu) + (jj)_Z^{0,1,2\,b\,tags} + (jj)_{VBF}$	6	230–1000 [c]	3%
	VBF tag	$(ee, \mu\mu) + (J)_Z^{0,1,2\,b\,tags} + (jj)_{VBF}$	6	230–1000 [c]	3%

[a]EW singlet model interpretation starts at 200 GeV to avoid contamination from h(125).
[b]600–1000 GeV for $\sqrt{s} = 8$ TeV only.
[c]For $\sqrt{s} = 8$ TeV only.

Table 1. A summary of the analyses included in this paper. The column "H production" indicates the production mechanism targeted by an analysis; it does not imply 100% purity in the selected sample. The main contribution in the untagged categories is always ggF. The $(jj)_{VBF}$ refers to a dijet pair consistent with the VBF topology. $(jj)_{W(Z)}$ and $(J)_{W(Z)}$ refer to a dijet pair and single merged jet from a Lorentz-boosted W (Z) with an invariant mass consistent with a W (Z) dijet decay, respectively. The superscript "0,1,2 b tags" refers to the three possible categories of b tag multiplicities. Exclusive final states are selected according to the lepton and reconstructed jet content of the event. The mass range under investigation and the mass resolution are also listed. Mass ranges differ with the sensitivities of each channel.

5 Data analysis

The results presented in this paper are obtained by combining searches exploiting different Higgs boson production and decay modes as detailed in table 1. All final states are exclusive, without overlap between channels. For the $WW \to \ell\nu\ell\nu$ and $ZZ \to 2\ell2\ell'$ channels a mass range starting from 110 GeV has been analyzed in other contexts (e.g. [12]), but in this paper both analyses are restricted to searches above 145 GeV . In the rest of this section, the individual analysis strategies and details are defined including a discussion of the leading systematic uncertainties. In the next section, statistical interpretations of the individual and combined searches are given for the Higgs boson with SM-like couplings hypothesis as well as the EW singlet extension of the SM.

5.1 H → WW → ℓνℓν

In the H → WW → ℓνℓν channel the Higgs boson decays to two W bosons, both of which decay leptonically, resulting in a signature with two isolated, oppositely charged, high-p_T leptons (muons or electrons) and large $E_\mathrm{T}^\mathrm{miss}$ due to the undetected neutrinos. A complete description of the analysis strategy is given in ref. [18]. For this analysis, we require triggers with either one or two high-p_T muons or electrons. The single muon or electron triggers are based on relatively tight lepton identification with p_T thresholds from 17 to 25 GeV (17 to 27 GeV) in the muon (electron) channel. The higher thresholds are used for periods of higher instantaneous luminosity. The dilepton trigger p_T thresholds for the leading and trailing leptons were 17 and 8 GeV, respectively.

Candidate events must contain two reconstructed leptons with opposite charge, $p_\mathrm{T} >$ 20 GeV for the leading lepton, and $p_\mathrm{T} > 10$ GeV for the subleading one. Only muons (electrons) with $|\eta| < 2.4\,(2.5)$ are considered in this channel. The analysis is very similar to that in the Higgs boson discovery [11, 12], but additionally uses an improved Higgs boson lineshape model.

Events are classified into three mutually exclusive categories, according to the number of reconstructed jets with $p_\mathrm{T} > 30$ GeV . The categories are characterized by different signal yields and signal-to-background ratios. In the following, these are referred to as 0-jet, 1-jet, and 2-jet multiplicity categories. Events with more than two jets are considered only if they are consistent with the VBF signature: a dijet mass of the two highest p_T jets greater than 500 GeV, $|\Delta\eta_\mathrm{jj}| > 3.5$, and no additional jets with $p_\mathrm{T} > 30$ GeV in the η region between these two leading jets. Signal candidates are further divided into same-flavor (SF) dilepton ($\mu^+\mu^-$ or e^+e^-) and different-flavor (DF) dilepton ($\mu^\pm e^\mp$) categories. The bulk of the signal arises through direct W boson decays to muons or electrons, with the small contribution from $W \to \tau\nu \to \ell + X$ decays implicitly included.

In addition to high-p_T isolated leptons and minimal jet activity, significant $E_\mathrm{T}^\mathrm{miss}$ is expected to be present in signal events, as opposed to none to moderate $E_\mathrm{T}^\mathrm{miss}$ in background. For this channel, an $E_\mathrm{T,\,pr}^\mathrm{miss}$ variable is employed, defined as (i) the magnitude of the $\vec{E}_\mathrm{T}^\mathrm{miss}$ component transverse to the closest lepton, if $\Delta\phi(\ell, \vec{E}_\mathrm{T}^\mathrm{miss}) < \pi/2$, or (ii) the magnitude of $\vec{E}_\mathrm{T}^\mathrm{miss}$ otherwise. This observable more efficiently distinguishes $Z/\gamma^* \to \tau^+\tau^-$ background events in which the $\vec{E}_\mathrm{T}^\mathrm{miss}$ is preferentially aligned with the leptons, and $Z/\gamma^* \to \ell^+\ell^-$ events with mismeasured $\vec{E}_\mathrm{T}^\mathrm{miss}$. Since the $E_\mathrm{T,\,pr}^\mathrm{miss}$ resolution is degraded as pileup increases, the minimum of two different observables is used: the first includes all particle candidates in the event, while the second uses only the charged particle candidates associated with the primary vertex. Events with $E_\mathrm{T,\,pr}^\mathrm{miss} > 20$ GeV are selected for this analysis.

The backgrounds are suppressed using techniques described in refs. [11, 12]. Top quark background is controlled with a selection based on the presence of a soft muon and b-jet tagging [105]. Rejection of events with a third lepton passing the same requirements as the two selected leptons reduces both WZ and Wγ^* backgrounds.

The Drell-Yan (DY) process produces SF lepton pairs ($\mu^+\mu^-$ and e^+e^-) and therefore additional requirements are applied for the SF final state. Firstly, the resonant component of the DY background is rejected by requiring a dilepton mass outside a 30 GeV window

centered on the Z boson mass. The remaining off-peak contribution is further suppressed by requiring significant missing transverse energy in the event. For the $\sqrt{s} = 7\,\text{TeV}$ data, we require $E_{\text{T, pr}}^{\text{miss}} > (37 + N_{\text{vtx}}/2)\,\text{GeV}$ directly, while for $\sqrt{s} = 8\,\text{TeV}$ data, a boosted decision tree (BDT) multivariate discriminant including $E_{\text{T, pr}}^{\text{miss}}$ is used. For events with two jets, the dominant source of misreconstructed $E_{\text{T}}^{\text{miss}}$ is the mismeasurement of the hadronic recoil, and optimal performance is obtained by requiring $E_{\text{T}}^{\text{miss}} > 45\,\text{GeV}$. Finally, the momenta of the dilepton system and of the most energetic jet must not be back-to-back in the transverse plane. For the $\sqrt{s} = 7\,\text{TeV}$ data, we require the angle to be less than 165 degrees , while for $\sqrt{s} = 8\,\text{TeV}$ data, this information is included in the BDT. These selections reduce the DY background by three orders of magnitude, while rejecting less than 50% of the signal.

The final analysis in the DF and in the SF 0-jet or 1-jet categories is performed using a two-dimensional fit in two observables, the dilepton invariant mass $m_{\ell\ell}$ and the transverse mass m_{T} determined between the transverse dilepton system, $\vec{p}_{\text{T}}^{\,\ell\ell}$, and the $\vec{E}_{\text{T}}^{\text{miss}}$:

$$m_{\text{T}} = \sqrt{2 p_{\text{T}}^{\ell\ell} E_{\text{T}}^{\text{miss}} \left(1 - \cos\Delta\Phi\left(\vec{p}_{\text{T}}^{\,\ell\ell}, \vec{E}_{\text{T}}^{\text{miss}}\right)\right)}, \tag{5.1}$$

where $\Delta\Phi(\vec{p}_{\text{T}}^{\,\ell\ell}, \vec{E}_{\text{T}}^{\text{miss}})$ is the azimuthal angle between the dilepton transverse momentum and the $\vec{E}_{\text{T}}^{\text{miss}}$.

Figure 1 shows the distributions of these two observables for the 0-jet DF category. The fit ranges in $m_{\ell\ell}$ and m_{T} are dependent on the m_{H} hypothesis. For $m_{\text{H}} > 200\,\text{GeV}$, additional selections requiring $p_{\text{T}} > 50\,\text{GeV}$ for the leading lepton and $m_{\text{T}} > 80\,\text{GeV}$ are imposed to suppress the h(125) contribution. A cross-check counting analysis is performed by applying selection criteria to several kinematic observables including $m_{\ell\ell}$ and m_{T}.

For the VBF production mode [107–110], the cross section is roughly ten times smaller than for ggF at lower m_{H} hypotheses and is roughly three times smaller at the highest m_{H} hypothesis. We optimize the selection in the 2-jet category to tag these VBF-type events by requiring the mass of the dijet system to fulfill $m_{\text{jj}} > 500\,\text{GeV}$, and the angular separation of the two jets to pass $|\Delta\eta_{\text{jj}}| > 3.5$. Given the small event yield in this category, the signal extraction in the DF category is performed using a one-dimensional fit in $m_{\ell\ell}$ where an m_{H} dependent requirement on the transverse mass is imposed. A counting analysis is performed in the SF category and is used as a cross-check in the DF category.

The normalization of the background contributions relies on observed events rather than simulation whenever possible, and exploits a combination of techniques [11, 12]. The $t\bar{t}$ background is estimated by extrapolation from the observed number of events with the b-tagging requirement inverted. The DY background measurement is based on extrapolation from the observed number of $\mu^+\mu^-$ and e^+e^- events with the Z boson veto requirement inverted. The background of W + jets and Quantum Chromodynamics (QCD) multijet events is estimated by measuring the number of events with one loosely isolated lepton. The probability for such loosely isolated nongenuine leptons to pass the tight isolation criteria is measured in observed data using multijet events. In the 0-jet and 1-jet bins, the nonresonant WW contribution is estimated from a fit to the data while in the 2-jet
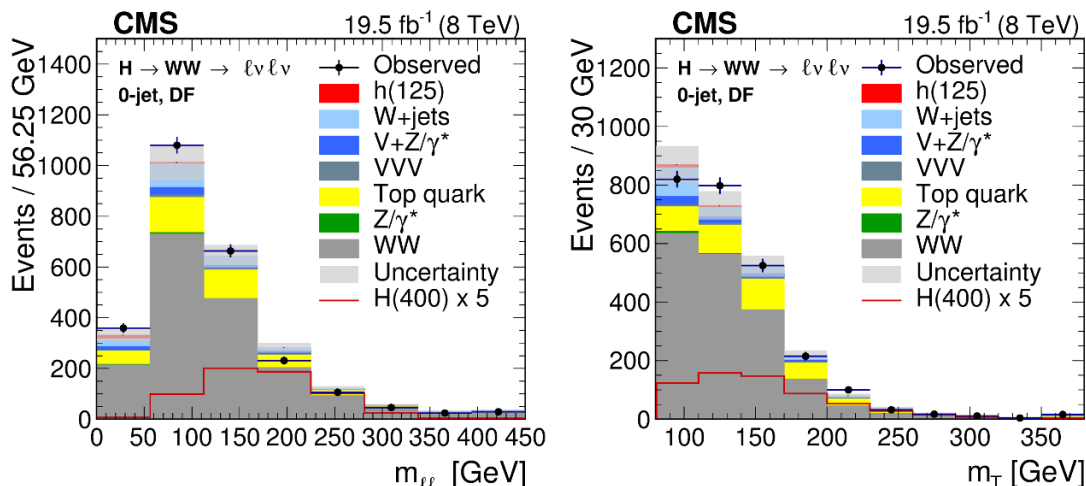
Figure 1. Distributions of $m_{\ell\ell}$ (left) and m_T (right) for the 0-jet DF category of the $H \to WW \to \ell\nu\ell\nu$ search. The uncertainty in the background histograms includes the systematic uncertainties on all background estimates and is centered on the sum of all backgrounds, including the h(125) in red. The W + jets distributions include the contributions from QCD multijet processes as well. The red open histogram shows five times the expectation for a $m_H = 400\,\mathrm{GeV}$ SM-like Higgs boson. The selection has been optimized to suppress the h(125) contribution as explained in the text.

bin it is estimated from simulation. Other backgrounds, such as $V+Z/\gamma^*$ and triple boson production (VVV) are estimated from simulation and are small.

Experimental effects, theoretical predictions, and the choice of event generators (POWHEG, GG2WW, MADGRAPH, PHANTOM) are considered as sources of systematic uncertainty, and their impact on the signal efficiency is assessed. The overall signal normalization uncertainty is estimated to be about 20%, and is dominated by the theoretical uncertainty associated with missing higher-order QCD corrections and PDF uncertainties, estimated following the PDF4LHC recommendations [81, 111–114]. The total uncertainty in the background estimation in the $H \to WW$ signal region is about 15% and is dominated by the statistical uncertainty in the observed number of events in the background control regions.

5.2 $H \to WW \to \ell\nu qq$

5.2.1 Unmerged-jet category

In the $H \to WW \to \ell\nu qq$ channel we search for a Higgs boson decaying to WW, where one W decays leptonically, thus providing a trigger handle for the event, while the other decays hadronically. This channel has a larger branching fraction than the two-lepton final state and allows one to reconstruct the Higgs boson candidate invariant mass [115]. The final state consists of an isolated electron or muon, E_T^{miss}, and two separated jets. The main experimental challenge is to control the large W+jets background.

We use data collected with a suite of single-lepton triggers mostly using p_T thresholds of 24 (27) GeV for muons (electrons). Basic kinematic selections are applied to the

final-state objects to reduce the background contribution. The muon (electron) is required to be isolated and have $p_{\mathrm{T}} > 25\,(35)\,\mathrm{GeV}$. A veto is imposed on additional muons and electrons in the event to reduce backgrounds from DY events. The events are required to have $E_{\mathrm{T}}^{\mathrm{miss}} > 25\,(30)\,\mathrm{GeV}$ in case of muons (electrons). The transverse mass $m_{\mathrm{T}} = \sqrt{2p_{\mathrm{T}} E_{\mathrm{T}}^{\mathrm{miss}}(1 - \cos\Delta\Phi)}$, with $\Delta\Phi$ being the azimuthal angle between the lepton p_{T} and $\vec{E}_{\mathrm{T}}^{\mathrm{miss}}$, needs to be greater than $30\,\mathrm{GeV}$. The two leading-p_{T} jets in the event each must have $p_{\mathrm{T}} > 30\,\mathrm{GeV}$ and must together have an invariant mass, m_{jj}, between 66 and $98\,\mathrm{GeV}$. An unbinned maximum likelihood fit is performed on m_{jj} to determine the background normalizations in the signal region for each Higgs mass hypothesis independently. Events that contain a b-tagged jet are vetoed in order to reduce the background from top quark decays.

To further exploit the differences in kinematics between the signal and background, a likelihood discriminant is constructed using angles between the Higgs boson decay products that fully describe the Higgs boson production kinematics [19, 71] and the lepton charge. The lepton charge provides discrimination power because of the charge asymmetry in the background, which is not present in the signal. This approach improves the expected sensitivity to a Higgs boson across the entire mass range.

The background normalization in the signal region is extracted for each Higgs boson mass hypothesis independently with an unbinned maximum likelihood fit to the dijet invariant mass distribution, m_{jj}, of the two leading jets. The signal region corresponding to the W boson mass window, $66 < m_{\mathrm{jj}} < 98\,\mathrm{GeV}$, is excluded from the fit. The background is overwhelmingly due to events from W+jets production. The normalization of the W+jets component is a free parameter and is determined in the fit. The electroweak diboson, $\mathrm{t\bar{t}}$, and single top shapes are based on simulation and their normalizations are constrained to the theoretical predictions with associated uncertainties. In the case of diboson backgrounds, both WW and WZ normalizations come from NLO predictions. The uncertainties in the normalization of the W+jets component obtained from the fit, as well as those from all other backgrounds, are included in the limit calculation as systematic uncertainties.

For the signal search, we use the binned distribution of m_{WW}, which is computed using a neutrino longitudinal momentum, p_z, that is determined from the constraint that the leptonically decaying W boson is produced on-shell. The ambiguity of two possible solutions is resolved by taking the solution that yields the smaller $|p_z|$ value for the neutrino. According to simulation over 85% of signal events are assigned the correct p_z value, thus improving the mass resolution, especially at low Higgs mass. The contribution of each background in the signal region ($66 < m_{\mathrm{jj}} < 98\,\mathrm{GeV}$) is described by an expected shape and normalization. The distribution of the W+jets contribution is parameterized with a polynomial functional form determined through simulation. The parameters of the function are determined from the observed data spectrum in the binned likelihood fit, which is also used to determine the exclusion limits. The other background shape distributions are parameterized using simulation, and their normalizations and uncertainties are included as nuisance parameters. Figure 2 depicts the m_{WW} distribution for the muon category for two different Higgs boson mass hypotheses. The observed data are compared to background and signal expectations.
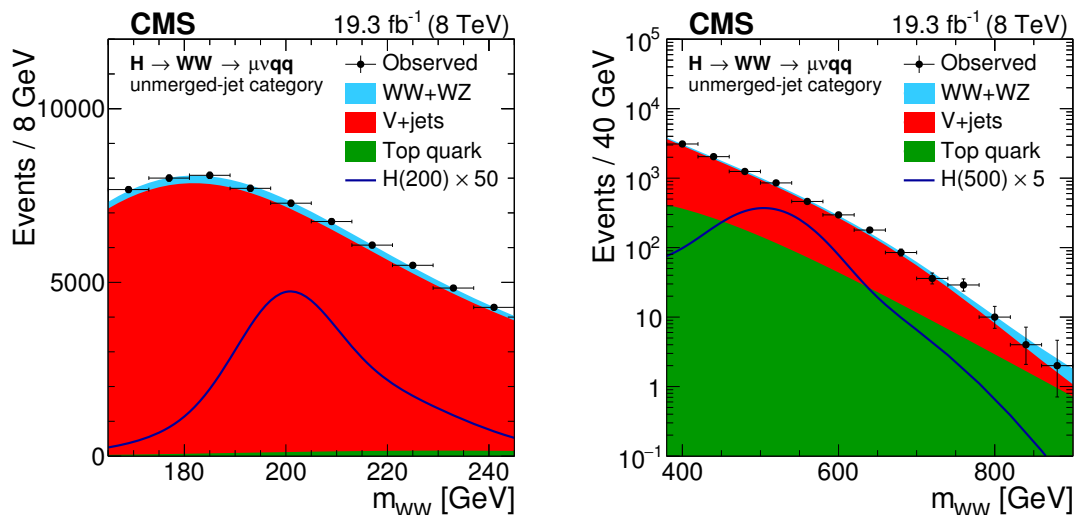
Figure 2. The WW invariant mass distribution with the fit projections in the signal region $66 < m_{jj} < 98$ GeV, for the muon channel of the unmerged-jet category. The V+jets background includes both, the large contribution from W+jets production, and the much smaller component of Z+jets. The blue curve on the left (right) shows 50 (5) times the expectation for a $m_H = 200$ (500) GeV SM-like Higgs boson.

Experimental effects, theoretical predictions, and uncertainties due to the choice of fit functions are considered as sources of systematic uncertainty. Because of the large background, the dominant source of systematic uncertainty is the shape uncertainty of the W+jets m_{WW} distribution, followed by the normalization uncertainty that is extracted from the m_{jj} fit. The main uncertainty in the signal normalization stems from the uncertainty in the efficiency of the likelihood discriminant selection. This effect occurs because of mismodeling of the likelihood discriminant and is studied in a signal-depleted region of the analysis.

5.2.2 Merged-jet category

In the highest mass range of this search, from 600 to 1000 GeV, the p_T of the decaying W bosons is typically greater than 200 GeV . At this p_T, the daughter quarks of the hadronically decaying W are often merged into a single jet to the point where traditional dijet searches cannot be performed. For a signal mass of 600 GeV (1 TeV), and signal events falling in the detector acceptance, approximately 65% (82%) of the hadronic W decay products are contained in a cone of $\Delta R < 0.8$; alternatively, approximately 10% (42%) of the hadronic W decay products are separated by a distance of $\Delta R < 0.5$ and would not be reconstructed by the standard CMS AK5 jet finding algorithm. The larger cone CA8 jet affords more signal acceptance in the single jet signature while not losing events when the decay products are separated by $\Delta R < 0.5$. In this case, we use jet substructure techniques for identifying jets that have originated from a hadronically decaying W boson with high Lorentz boost.

As in the unmerged case, we use data collected with the single electron or muon trigger. The dominant background is W+jets with a smaller background contribution from $t\bar{t}$. Remaining backgrounds arise from WW, WZ, ZZ, and single top quark production.

The hadronic W boson candidate is reconstructed with CA8 jets to increase acceptance. To reduce the contribution of quark- and gluon-initiated jets from QCD processes, a selection is made on the pruned jet mass of the CA8 jet of $65 < m_{\mathrm{J}} < 105\,\mathrm{GeV}$ and the N-subjettiness ratio $\tau_2/\tau_1 < 0.5$.

The kinematic selections of muons and electrons are slightly more stringent than those for the unmerged case, with the p_{T} thresholds of isolated muons and electrons being 30 and $35\,\mathrm{GeV}$, respectively. The $E_{\mathrm{T}}^{\mathrm{miss}}$ requirement is increased to be greater than 50 (70) GeV in the muon (electron) channel. The p_{T} of both, leptonically and hadronically decaying W boson candidates, is required to be greater than $200\,\mathrm{GeV}$ in order to select events with a large Lorentz boost. Additional selections are made to ensure that the W boson candidates are sufficiently separated in a back-to-back topology. As in the unmerged category, there is an additional requirement to veto events with a b tagged jet in order to reduce the background from top quark decays.

To increase the sensitivity of the analysis, the analysis is split into exclusive jet multiplicity categories: 0+1-jet and 2-jets. These additional AK5 jets must pass a p_{T} threshold of $30\,\mathrm{GeV}$ and be separated from the hadronic W candidate in the event by a distance $\Delta R > 0.8$. Additionally, the 2-jet category has further requirements to better identify a topology consistent with the VBF production mode. The two highest p_{T} AK5 jets in the event are required to satisfy $|\Delta\eta_{\mathrm{jj}}| > 2.5$ and $m_{\mathrm{jj}} > 250\,\mathrm{GeV}$. There is also a requirement on the invariant mass of the W boson candidates and the nearest AK5 jet to be greater than $200\,\mathrm{GeV}$ in order to reject other top quark background. The final discriminating distribution is the m_{WW} shape reconstructed from the lepton + $E_{\mathrm{T}}^{\mathrm{miss}}$ + CA8 jet system. Because the number of events in the 2-jet category is limited, the muon and electron datasets are merged.

The background is estimated using observed data rather than simulation wherever possible. The dominant W+jets background normalization is determined from a fit to the pruned jet mass sideband where other backgrounds contribute less significantly. The W+jets shape is determined from extrapolating the pruned jet mass sideband region into the signal region. The $t\bar{t}$ background is estimated by inverting the veto on AK5 b-tagged jets, which yields a high-purity $t\bar{t}$ control sample. The normalization of $t\bar{t}$ in the signal region is then corrected by a data-to-MC scale factor determined from the $t\bar{t}$ control sample. Finally the $t\bar{t}$ control sample is also a good source of W bosons with high Lorentz boost, which are used to calibrate the jet substructure selection efficiency.

Figure 3 displays the final m_{WW} distributions after all selections and background estimations for the 0+1-jet category for the muon channel only on the left and for the 2-jet category on the right. In the 2-jet category, there is an excess observed around $750\,\mathrm{GeV}$ with local significances of $2.6\,\sigma$ at $700\,\mathrm{GeV}$ and $2.1\,\sigma$ at $800\,\mathrm{GeV}$. No such excess is observed in the 0+1-jet multiplicity bin.

Sources of systematic uncertainty are similar to the unmerged-jet category. The dominant experimental uncertainties are the background normalization and shape uncertainty, particularly in the 2-jet category, where the number of events is small, as well as the uncertainty in the signal cross section due to the hadronic W candidate selection. The dominant theoretical uncertainty comes from the uncertainty in the cross section when dividing the analysis into exclusive jet multiplicity bins.
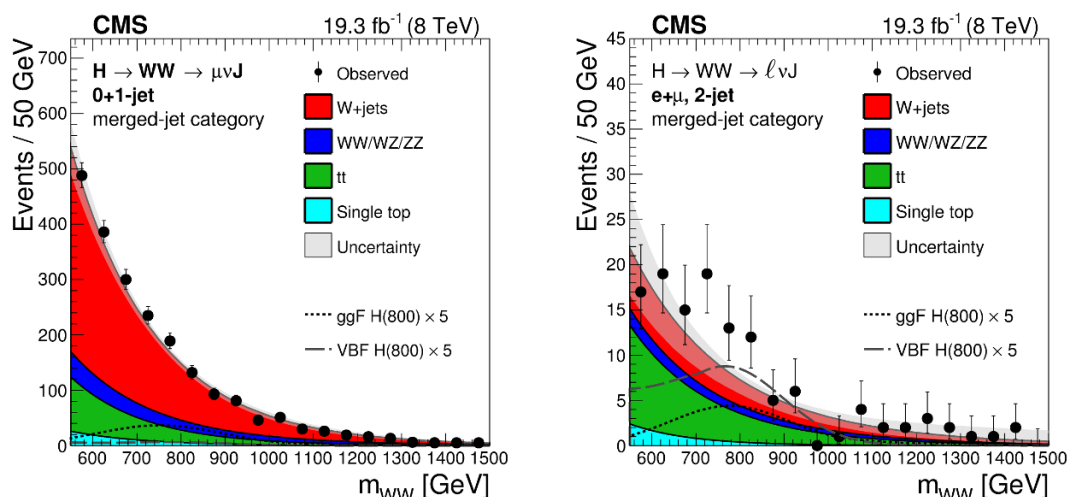
Figure 3. The final WW invariant mass distribution is shown for the 0+1-jet bin category for the muon channel only (left) and for the 2-jet bin category (right). Points represent the observed data, shaded graphs represent the background and dashed graphs represent five times the expectation for a $m_H = 800$ GeV SM-like Higgs boson from ggF and VBF production, separately.

5.3 $H \rightarrow ZZ \rightarrow 2\ell 2\ell`$

This analysis seeks to identify Higgs boson decays to a pair of Z bosons, with one Z decaying to a pair of muons or electrons ($Z \rightarrow 2\ell$, with $\ell = \mu$ or e), and the second decaying to electrons, muons or taus ($Z \rightarrow 2\ell`$, with $\ell` =$ e, μ or τ) [11, 19, 116]. This channel has extremely low background, and the presence of four leptons in the final state allows reconstruction and isolation requirements to be very loose, leading to a high selection efficiency. This channel is one of the most sensitive channels across the entire mass range.

For this analysis, we require triggers with two high-p_T muons or electrons. The dilepton trigger p_T thresholds for the leading and trailing leptons were 17 and 8 GeV, respectively. Events included in the analysis contain Z boson candidates formed from a pair of leptons of the same flavor and opposite charge. Decay muons or electrons are required to be isolated, and to originate from the primary vertex. Muons (electrons) are required to have $p_T > 5(7)$ GeV and $|\eta| < 2.1(2.5)$, while taus are required to have a visible transverse momentum $p_T > 20$ GeV and $|\eta| < 2.3$. We reconstruct the $Z \rightarrow \tau\tau$ in the following decay modes: $Z \rightarrow \tau_h\tau_h$, $Z \rightarrow \tau_e\tau_h$, $Z \rightarrow \tau_\mu\tau_h$, and $Z \rightarrow \tau_e\tau_\mu$. Overlap with the $2\ell 2\ell$ channel is avoided by excluding events with both taus decaying to electrons or muons.

For the $2\ell 2\ell$ final state, the lepton pair with invariant mass closest to the nominal Z boson mass, denoted Z_1, is identified and retained if $40 < m_{Z_1} < 120$ GeV . The second Z boson, denoted Z_2, is then constructed from the remaining leptons in the event, and is required to satisfy $12 < m_{Z_2} < 120$ GeV . If more than one Z_2 candidate remains, the ambiguity is resolved by choosing the leptons of highest p_T. Amongst the four candidate decay leptons, at least one should have $p_T > 20$ GeV, and another should have $p_T > 10$ GeV. This requirement ensures that selected events correspond to the high-efficiency plateau of the trigger.

For the $2\ell 2\tau$ final state, events are required to have one $Z_1 \to 2\ell$ candidate, with one lepton having $p_T > 20\,\mathrm{GeV}$ and the other $p_T > 10\,\mathrm{GeV}$. The leptons from leptonic decays of the tau are required to have $p_T > 10\,\mathrm{GeV}$. The invariant mass of the reconstructed Z_1 candidate is required to satisfy $60 < m_{\ell\ell} < 120\,\mathrm{GeV}$. The Z_2 candidate mass reconstructed from the visible tau decay products (visible mass), $m_{\tau\tau}$, must satisfy $30 < m_{\tau\tau} < 90\,\mathrm{GeV}$ for events with at least one hadronically decaying tau, and $20 < m_{\tau\tau} < 90\,\mathrm{GeV}$ for events with two leptonically decaying taus. Events with both taus decaying to muons or electrons are excluded in order to avoid overlap with the $2\ell 2\ell$ channel. The selections on the reconstructed Z_1 mass for the $2\ell 2\tau$ final state are tighter than for the $2\ell 2\ell$ channel, because the search range starts at $m_H = 200\,\mathrm{GeV}$ rather than $m_H = 145\,\mathrm{GeV}$.

In order to further separate signal from background and to distinguish different signal production mechanisms, we use a matrix element likelihood approach, which relies on probabilities for an event to come either from signal or background using a set of observables, such as angular and mass information, which fully characterize the event topology in its center-of-mass frame [71].

The events are categorized according to their jet multiplicity, counting jets with $p_T > 30\,\mathrm{GeV}$. In the 0- or 1-jet category the p_T spectrum of the four-lepton system is exploited to distinguish between ggF and vector boson induced production modes, such as VBF and associated production with a vector boson (VH). The events selected with two or more jets potentially come from several sources: background (predominantly ZZ+2 jets), VBF signal, VH signal (with V→2 jets), and ggF signal gg → H+2 jets. In order to isolate the production mechanism, we use a matrix-element-based probability [71, 117] for the kinematics of the two jets and the Higgs boson to come either from the VBF process or from the gg → H+2 jets process. This discriminant is equally efficient to separate VBF from either H+2 jets signal or ZZ+2 jets background, because both processes show very similar jet kinematics.

To allow estimation of the $t\bar{t}$, Z+jets, and WZ+jets backgrounds, a Z_1+X control region is defined, well separated from the expected signal region. In addition, a sample of $Z_1+\ell$ events, with at least one reconstructed lepton in addition to a Z, is defined in order to estimate the lepton misidentification probability, which is the probability for non-prompt leptons and other particles, which are not leptons, to be reconstructed as leptons and to pass the isolation and identification requirements. The contamination of the sample from WZ events containing a genuine additional lepton is suppressed by requiring the energy imbalance measured in the transverse plane to be below $25(20)\,\mathrm{GeV}$ for the $2\ell 2\ell$ ($2\ell 2\tau$) channel. The event rates measured in the background control region are extrapolated to the signal region. The systematic uncertainties associated with the reducible background estimate vary from 30% to 100% and are combined in quadrature with the statistical uncertainties.

The cross section for ZZ production at NLO is calculated with MCFM. The theoretical uncertainty in the cross section is evaluated as a function of $m_{2\ell 2\ell'}$, varying both the renormalization and factorization scales and the PDF set, following the PDF4LHC recommendations [81, 111–114].

The reconstructed invariant mass distribution for $2\ell 2\ell$, combining the 4μ, 2μ2e, and 4μ channels, is shown in figure 4 (left), compared with the expectation from SM background
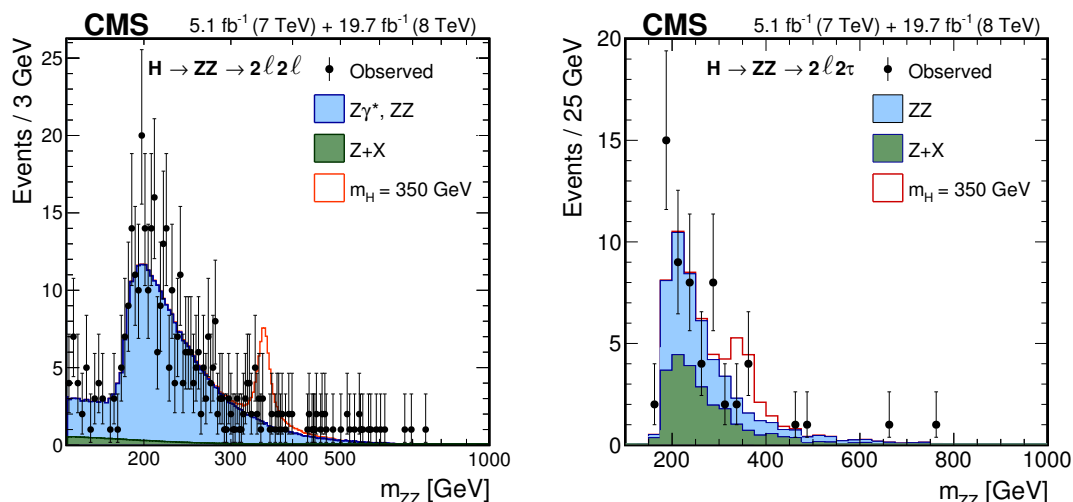
Figure 4. Distribution of the four-lepton reconstructed mass for the sum of the 4μ, $2\mu2e$, and $4e$ channels (left), and for the sum over all $2\ell2\tau$ channels (right). Points represent the observed data, shaded histograms represent the background, and the red open histogram shows the expectation for a $m_{\mathrm{H}} = 350\,\mathrm{GeV}$ SM-like Higgs boson.

processes. Figure 4 (right) plots the reconstructed visible mass distribution for the $2\ell2\tau$ selection, combining all $2\ell2\tau$ final states.

The background shapes are taken from simulation, with rates normalized to the observed data. The measured Z boson and ZZ masses are underestimated due to the undetected neutrinos in tau decays. To compensate for this effect we correct the momenta of the visible tau decay products to constrain the Z boson mass to $91.2\,\mathrm{GeV}$. The correction is applied on the selected events and only affects the final mass shape of the ZZ system. The observed mass distributions are well-matched to the SM background expectation.

In the $2\ell2\ell$ channel limits on the production of heavy Higgs bosons are extracted using the unbinned four lepton mass distribution and the correlation of the kinematic discriminant with the Higgs boson mass. In the case of the tagged 2-jet category a third dimension is introduced using the correlation of the aforementioned VBF discriminant with the four-lepton mass. In the untagged 0/1-jet category the transverse momentum of the four lepton system is used in place of the VBF discriminant. For the $2\ell2\tau$ final state, limits are set using the $m_{2\ell2\tau}$ distribution.

5.4 H → ZZ → $2\ell2\nu$

This analysis seeks to identify Higgs boson decays to a pair of Z bosons, with one Z boson decaying to neutrinos and the other decaying to leptons. The analysis strategy is based on selection requirements in the ($E_{\mathrm{T}}^{\mathrm{miss}}$, m_{T}) phase space, with selections adjusted for different m_{H} hypotheses [118]. Here, the transverse mass is determined between the transverse dilepton system, $\vec{p}_{\mathrm{T}}^{\,\ell\ell}$, and the $\vec{E}_{\mathrm{T}}^{\mathrm{miss}}$.

As in the previous section, we use data collected with the trigger requiring two high-p_{T} electrons or muons. Events are required to have a pair of well-identified, isolated leptons of

same flavor ($\mu^+\mu^-$ or e$^+$e$^-$), each lepton with $p_\mathrm{T} > 20\,\mathrm{GeV}$, with an invariant mass within a 30 GeV window centered on the Z boson mass. The p_T of the dilepton system is required to be greater than 55 GeV. The presence of large $E_\mathrm{T}^\mathrm{miss}$ (70 GeV or more, depending on m_H) in the event is also required.

To suppress the Z+jets background, events are rejected if the angle in the transverse plane between the $\vec{E}_\mathrm{T}^\mathrm{miss}$ and the closest jet with $p_\mathrm{T} > 30\,\mathrm{GeV}$ is smaller than 0.5 radians. Events where the lepton is mismeasured are rejected if $E_\mathrm{T}^\mathrm{miss} > 60\,\mathrm{GeV}$ and $\Delta\phi(\ell, \vec{E}_\mathrm{T}^\mathrm{miss})$ < 0.2. The top quark background is suppressed by applying a veto on events having a b tagged jet with $p_\mathrm{T} > 30\,\mathrm{GeV}$ and $|\eta| < 2.5$. To further suppress this background, a veto is applied on events containing an additional, soft muon with $p_\mathrm{T} > 3\,\mathrm{GeV}$, typically produced in the leptonic decay of a b quark. To reduce the WZ background, in which both bosons decay leptonically, any event with a third lepton (μ or e) with $p_\mathrm{T} > 10\,\mathrm{GeV}$, and passing the identification and isolation requirements, is rejected.

The search is carried out in two mutually exclusive categories. The VBF category contains events with two or more jets in the forward region, with a $|\Delta\eta_\mathrm{jj}| > 4$ requirement between the two leading jets, and with the invariant mass of those two jets greater than 500 GeV . In addition, the two leptons forming the Z candidate are required to lie between these two jets in η, while no other selected jets with $p_\mathrm{T} > 30\,\mathrm{GeV}$ are allowed in this region. The ggF category includes all events failing the VBF selection, and is subdivided into subsamples according to the presence or absence of reconstructed jets with $p_\mathrm{T} > 30\,\mathrm{GeV}$. The event categories are chosen in order to maximize the expected cross section limit. In the case of the VBF category, a constant $E_\mathrm{T}^\mathrm{miss} > 70\,\mathrm{GeV}$ and no m_T requirement are used, as no gain in sensitivity is obtained with a selection dependent on the Higgs boson mass hypothesis. In the case of ggF, we apply an m_H-dependent lower limit on $E_\mathrm{T}^\mathrm{miss}$ ranging from 80 to 100 GeV over the search range.

The background composition is expected to vary with the m_H hypothesis. At low-m_H, Z+jets and $t\bar{t}$ processes are the largest contributions, while at $m_\mathrm{H} > 400\,\mathrm{GeV}$ the irreducible ZZ and WZ backgrounds dominate. The ZZ and WZ backgrounds are estimated from simulation and are normalized to their respective NLO cross sections. The Z+jets background is modeled from a control sample of events with a single photon produced in association with jets. This procedure yields a good model of the $E_\mathrm{T}^\mathrm{miss}$ distribution in Z+jets events.

The uncertainty associated with the Z+jets background is affected by residual contamination of the γ+jets control sample from processes involving a photon and genuine $E_\mathrm{T}^\mathrm{miss}$. We do not explicitly subtract this contamination, but include a shape uncertainty in the final fit, which is allowed to vary this small residual background between 0 and 100% of this estimate.

Background processes that do not involve a Z boson (nonresonant background), include $t\bar{t}$, single top quark production, W+jets and WW, and are estimated with a control sample of DF dilepton events ($\mu^\mp$e$^\pm$) that pass the full event selection. This method cannot distinguish between the nonresonant background and a possible contribution from H $\rightarrow$ WW $\rightarrow 2\ell2\nu$ events, which are treated as part of the nonresonant background estimate. The nonresonant background in the $\mu^+\mu^-$ or e$^+$e$^-$ final states is estimated by applying a
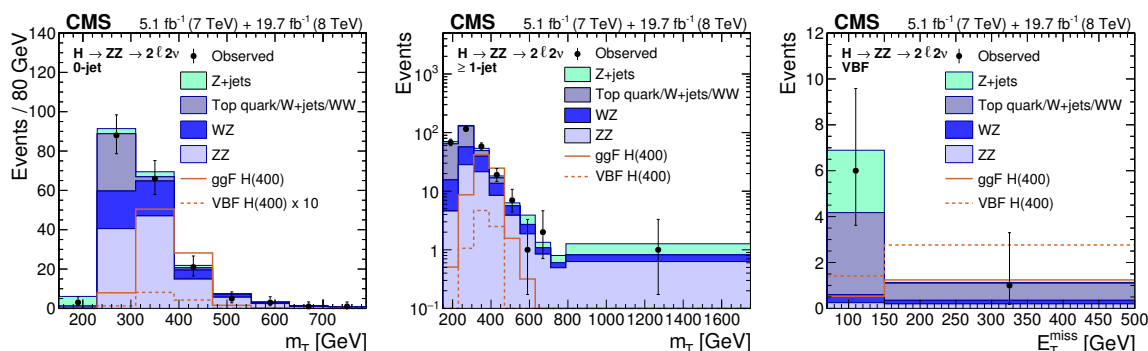
Figure 5. The final transverse mass (left, center) and missing transverse energy (right) distributions are shown for all three event categories of the H → ZZ → 2ℓ2ν channel: (left) events with zero jets, (center) events with at least one jet, but not passing the VBF selection, (right) VBF events. The expected distributions from the different background processes are stacked on top of each other. The red open histograms show the expectation for a $m_H = 400$ GeV SM-like Higgs boson separating the ggF and VBF contributions. In the case of the 0-jet category, the VBF contribution is multiplied by a factor of 10 to increase visibility.

scale factor to the selected $\mu^{\pm}e^{\mp}$ events, obtained from the events in the sidebands of the Z boson peak ($40 < m_{\ell\ell} < 70$ GeV and $110 < m_{\ell\ell} < 200$ GeV). The uncertainty associated with the estimate of this background is determined to be 25%. No significant excess of events is observed over the SM background expectation.

The m_T and E_T^{miss} distributions used to extract the results are shown in figure 5 for all three event categories with the muon and electron channels combined.

5.5 H → ZZ → 2ℓ2q

The H → ZZ → 2ℓ2q channel has the largest branching fraction of all H → ZZ channels under consideration, but also a large background contribution from Z+jets production. Furthermore, the reconstruction of the hadronically decaying Z boson is more difficult than the fully leptonic final states. The dominant background is due to the DY process and can be reduced using b-tagging requirements on the selected jets, as will be described later in this section.

As in the other channels with a Z boson in the final state, we use data collected with the trigger requiring two high-p_T muons or electrons. Reconstructed muons and electrons are required to have $p_T > 40(20)$ GeV for the leading (second) lepton. Muons are required to have $|\eta| < 2.4$, and electrons $|\eta| < 2.5$. Jets are required to have $p_T > 30$ GeV and $|\eta| < 2.4$. Each pair of oppositely charged leptons of the same flavor and each pair of jets are considered as Z boson candidates.

To increase the sensitivity to a possible signal, the main analysis is complemented with dedicated selections for the VBF signature. VBF events are identified requiring two additional jets with $p_T > 30$ GeV, $m_{jj} > 500$ GeV, and $|\Delta\eta_{jj}| > 3.5$.

Analogously to the H → WW → ℓνqq channel, the analysis is modified for very high Higgs boson masses ($m_H > 600$ GeV) to account for the fact that the two jets originate from

a Lorentz-boosted Z boson and therefore they may be reconstructed as a single, merged jet (sections 4 and 5.2.2). Information about the internal structure of this kind of jet [103] is used in order to gain some insight about the origin of the jet, distinguishing the DY background from jets produced from boosted Z bosons. To reduce the contamination from nonboosted Z + X backgrounds, the selection for the merged-jet topology requires the hadronically decaying Z boson to have $p_{\mathrm{T}} > 100\,\mathrm{GeV}$ and $|\eta| < 2.4$, and the leptonically decaying Z boson to have $p_{\mathrm{T}} > 200\,\mathrm{GeV}$.

In order to exploit the different jet composition of signal and background, events are classified into three mutually exclusive categories according to the number of selected b tagged jets: 0 b tag, 1 b tag, and 2 b tag. This distinction is not done in the VBF oriented selection where the main discrimination is given by a multivariate discriminator for VBF topology based on angular and energy information of the two VBF tag jets.

Background contributions are reduced by requiring $71 < m_{\mathrm{jj}} < 111\,\mathrm{GeV}$ and $76 < m_{\ell\ell} < 106\,\mathrm{GeV}$ in the selected events. The presence of Z bosons decaying to leptons and dijets makes this selection very efficient for signal, whereas the continuous background gets largely reduced. In case of the merged-jet analysis, the dijet requirement is applied on the merged-jet mass, after applying the pruning procedure.

An angular likelihood discriminant is used to separate signal-like from background-like events in each category [71, 119]. In order to suppress the substantial expected $t\bar{t}$ background in the 2 b tag category, a discriminant is used, defined as the logarithm of the likelihood ratio of the hypothesis that the $E_{\mathrm{T}}^{\mathrm{miss}}$ is equal to the value measured by the PF algorithm and the null hypothesis $E_{\mathrm{T}}^{\mathrm{miss}} = 0$ [91]. This discriminant provides a measure of whether the event contains genuine missing transverse energy. When an event contains multiple Z boson candidates passing the selection requirements, those with jets in the highest b tag category are retained for analysis. If multiple candidates are still present, the ones with m_{jj} and $m_{\ell\ell}$ values closest to the Z boson mass are retained. In the case of the merged-jet category all the requirements on jets with respect to b tagging and the likelihood discriminant are applied to the two subjets reconstructed inside the merged jet. In case of events with a merged-jet Z boson candidate in addition to a dijet one, the candidate from the merged jet gets selected.

The dominant Z+jets background is estimated using simulated events properly corrected to reproduce the yield of the observed data in the control regions, defined as $60 < m_{\mathrm{jj}} < 71\,\mathrm{GeV}$ and $111 < m_{\mathrm{jj}} < 130\,\mathrm{GeV}$. Simulated events are weighted to reproduce the p_{T} spectrum of the $\ell\ell\mathrm{jj}$ system in these control regions. In case of the merged-jet category both the p_{T} of the $\ell\ell$ and $\ell\ell\mathrm{J}$ systems have weights applied. The normalization of this distribution is taken from observed data and used as an additional constraint for this background.

Other backgrounds are estimated using simulated events. These include diboson and top quark events. In the VBF selection, the background from top quark events is small. In the ggF analysis it is estimated from observed data using a control sample of eμ events, invoking lepton flavor symmetry that is satisfied by several background contributions but not in the signal events.

The distributions of m_{ZZ} in the signal region are shown in figure 6 for the three b tag multiplicities of the dijet category comparing observed data with background expectations.
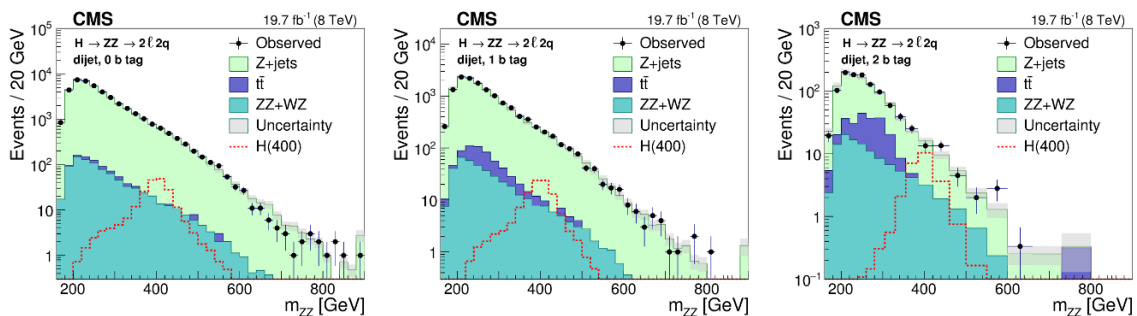
Figure 6. The m_{ZZ} invariant mass distribution after final selection in three categories of the H → ZZ → 2ℓ2q dijet channel: 0 b tag (left), 1 b tag (center), and 2 b tag (right). Points with error bars show distributions of observed data. Solid histograms are depicting the background expectation from simulated events for the different components. The red open histogram shows the expectation for a $m_H = 400\,\text{GeV}$ SM-like Higgs boson.

Good agreement is observed within the uncertainties. For the merged and VBF categories good agreement is also observed. The dominant systematic uncertainties are due to the b-tagging performance and the JES [97]. Further systematic effects are due to the uncertainty in the predicted signal and background shapes used in the analysis. The distributions of m_{ZZ} in the signal region are used to extract the final signal and background yields.

5.6 Systematic uncertainties

Systematic uncertainties for the various final states come from common treatment of the signal model assumptions, reconstructed objects used in the analysis and a few common experimental effects.

Uncertainties on the cross section for the production of heavy Higgs bosons arise from uncertainties in the combined choice of the PDFs and α_s, as well as in the renormalization and factorization scales [73], which are typically 6–7% and 7–12%, respectively, for the ggF production mechanism, and 1–2% and 2–5%, respectively, for production via VBF. Additionally, we add an uncertainty in the background coming from off-shell h(125) production, which we estimate with GG2ZZ (PHANTOM) for the ggF (VBF) case. We find that at the largest m_H values, the size of the effect is approximately 3% of the total background. Uncertainties on the signal lineshape reweighting with interference varies for the ggF and VBF modes. For ggF, we follow the prescription in ref. [73], which considers the NNLO contribution to the signal interfering with the gg → ZZ background process. For VBF, without a full prescription, we assign systematic uncertainties coming from renormalization and factorization scale variations in the PHANTOM generator.

Other common systematic effects come from the luminosity uncertainty, which is 2.2% (2.6%) for the 7 (8) TeV data. Uncertainties on the muon and electron reconstruction efficiencies, and JES and jet energy resolution (JER) are correlated among the various final states, where all these effects are subdominant. The lepton fake rate is largest for the H → ZZ → 2ℓ2ℓ' channel, in which we consider fake leptons at relatively lower p_T than in the other channels. A summary of the systematic uncertainties per channel is given in table 2.

Source of uncertainty	$H \to WW$ $\to \ell\nu\ell\nu$	$H \to WW$ $\to \ell\nu jj$	$H \to WW$ $\to \ell\nu J$	$H \to ZZ$ $\to 2\ell2\ell'$	$H \to ZZ$ $\to 2\ell2\nu$	$H \to ZZ$ $\to 2\ell2q$
Experimental sources						
Luminosity, 7 (8) TeV	2.2 (2.6)	2.2 (2.6)	2.2 (2.6)	2.2 (2.6)	2.2 (2.6)	2.2 (2.6)
ℓ trigger, reco, id, iso	1–4	1–2	1–2	0.5–7	2–3	1.8–2
ℓ mom./energy scale	2–4			0.5–30	1–2	0.1–0.4
ℓ misid. rate				30		
JES, JER, E_T^{miss}	2–35	<1	2	5–30	1	1–13
Pileup		<1			1–3	1
b-tag/mistag			2.5		1–3	1–6
W-tag/Z-tag			7.5			0–9.3
Signal selection eff.		10	2			
Monte Carlo statistics	1–20				1–2	0–6
Background estimates						
$t\bar{t}$, tW	20	7	6–30		25	0–15
Z+jets	40–100			20–42	100	16
ZZ	3			13–14	12	
W+jets	40	0.6	8		25	
WW	8–30	10	30		25	
WZ, Wγ^*	3–50		30		5.8–8.5	
Theoretical sources						
$\sigma(gg \to H)$	10–13	10–11	11–13	10–13	10–13	10–13
$\sigma(qq \to H)$	2.6–5.8	2.6–3.6	3.6–5.8	2.6–5.8	2.6–5.8	2.6–5.8
H lineshape				5	2–8	0–7
H–WW (ZZ) interference	1–27		10–50		10–50	
Jet binning	7–35		7–35		30	

Table 2. Sources of systematic uncertainties considered in each of the channels included in this analysis. Uncertainties are given in percent. Most uncertainties are affecting the normalisation of the observed data or simulated events, but some are uncertainties on the shape of kinematic distributions. Wherever ranges of uncertainties are given, they are either ranges in m_H, jet multiplicity categories, or dependent on the production mode.

6 Statistical interpretation

The combination of the measurements in the different channels presented in this paper requires the simultaneous analysis of the data selected by all individual analyses, accounting for all statistical and systematic uncertainties, as well as their correlations. The statistical methodology used in this combination was developed by the ATLAS and CMS Collaborations in the context of the LHC Higgs Combination Group [12, 120, 121]. Upper limits on the model parameters are set for different m_H hypotheses using a modified frequentist method referred to as the CL$_s$ method [122, 123], where a likelihood ratio test statistic is
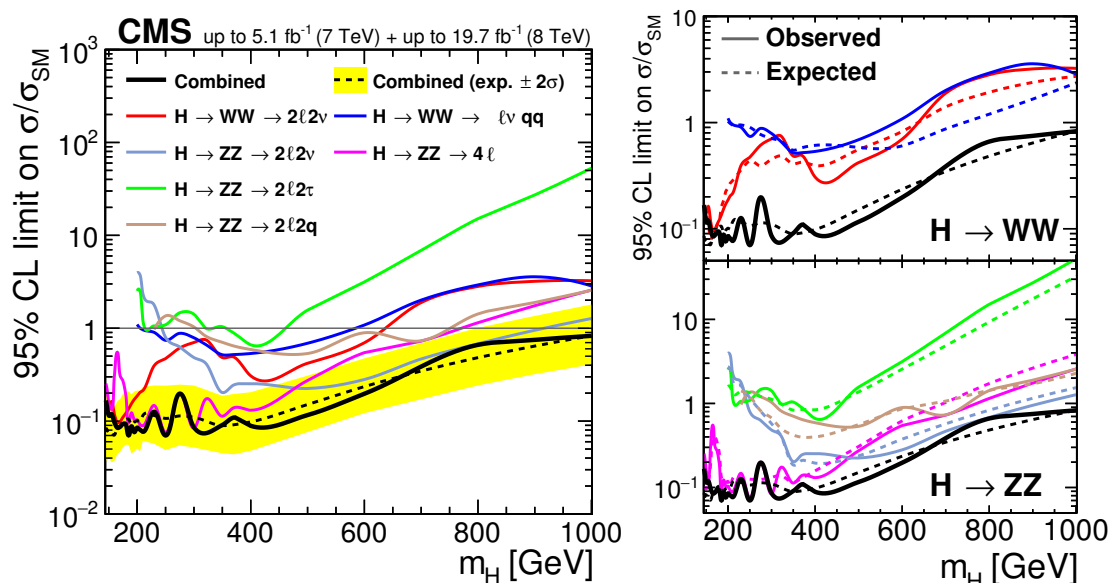
Figure 7. Upper limits at the 95% CL for each of the contributing final states and their combination. The theoretical cross section, σ_{SM}, is computed in ref. [73]. The observed and expected limits of the six individual channels are compared with each other and with the combined results (right), for $\mathrm{H} \to \mathrm{WW}$ channels (top right panel) and $\mathrm{H} \to \mathrm{ZZ}$ channels (bottom right panel) separately.

used in which the nuisance parameters are profiled. In the likelihood ratio, the total number of observed events is compared to the signal and background predictions by means of a product of Poisson probabilities. The predictions are subject to the multiple uncertainties described in the previous section, and are handled by introducing nuisance parameters with probability density functions. The nuisance parameters modify parametrically the expectations for both signal and background processes. Furthermore, a signal strength modifier (μ) is used to scale the Higgs boson cross sections of all production mechanisms by the same factor with respect to their SM predictions while keeping the decay branching fractions unchanged.

6.1 SM-like Higgs boson search

The combined results obtained for a heavy Higgs boson with SM-like couplings for all the different contributing final states are displayed in figure 7. On the left, the observed 95% CL limit is shown for each final state. The expected combined 95% CL limit of the six channels is plotted as a dashed black line, while the yellow shaded region is the $\pm 2\sigma$ uncertainty in the expected limit. On the right, the expected and observed limits are displayed for each of the individual channels as well as the combined result. The top right panel shows the WW final states, while the ZZ final states are displayed in the bottom right panel. In the lower mass region of the search range, the most sensitive channels are $\mathrm{H} \to \mathrm{ZZ} \to 4\ell$ and $\mathrm{H} \to \mathrm{WW} \to 2\ell 2\nu$. At the highest masses, the $\mathrm{H} \to \mathrm{ZZ} \to 2\ell 2\nu$ channel has the best sensitivity, while $\mathrm{H} \to \mathrm{ZZ} \to 4\ell$, $\mathrm{H} \to \mathrm{WW} \to 2\ell 2\nu$, $\mathrm{H} \to \mathrm{WW} \to \ell\nu\mathrm{qq}$, and $\mathrm{H} \to \mathrm{ZZ} \to 2\ell 2\mathrm{q}$ contribute significantly.
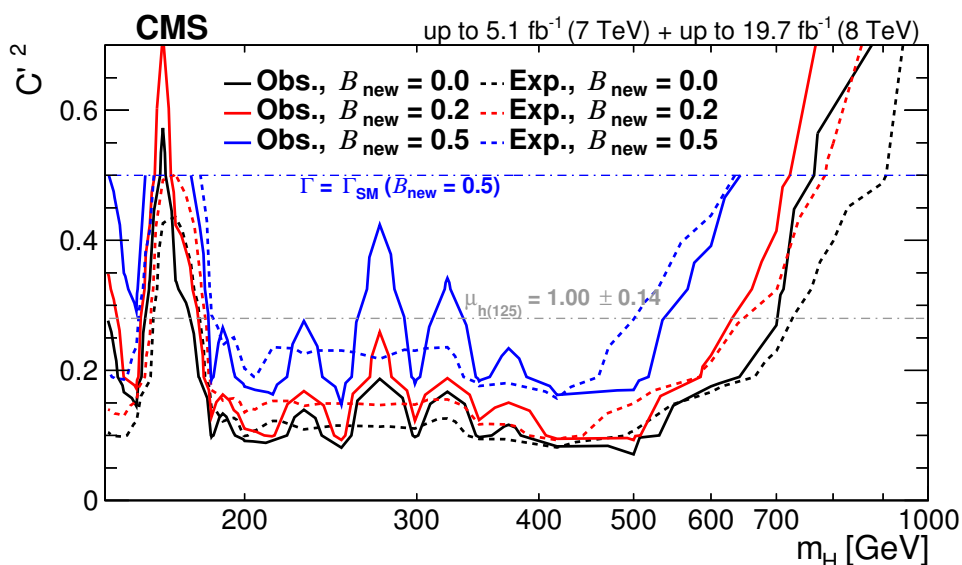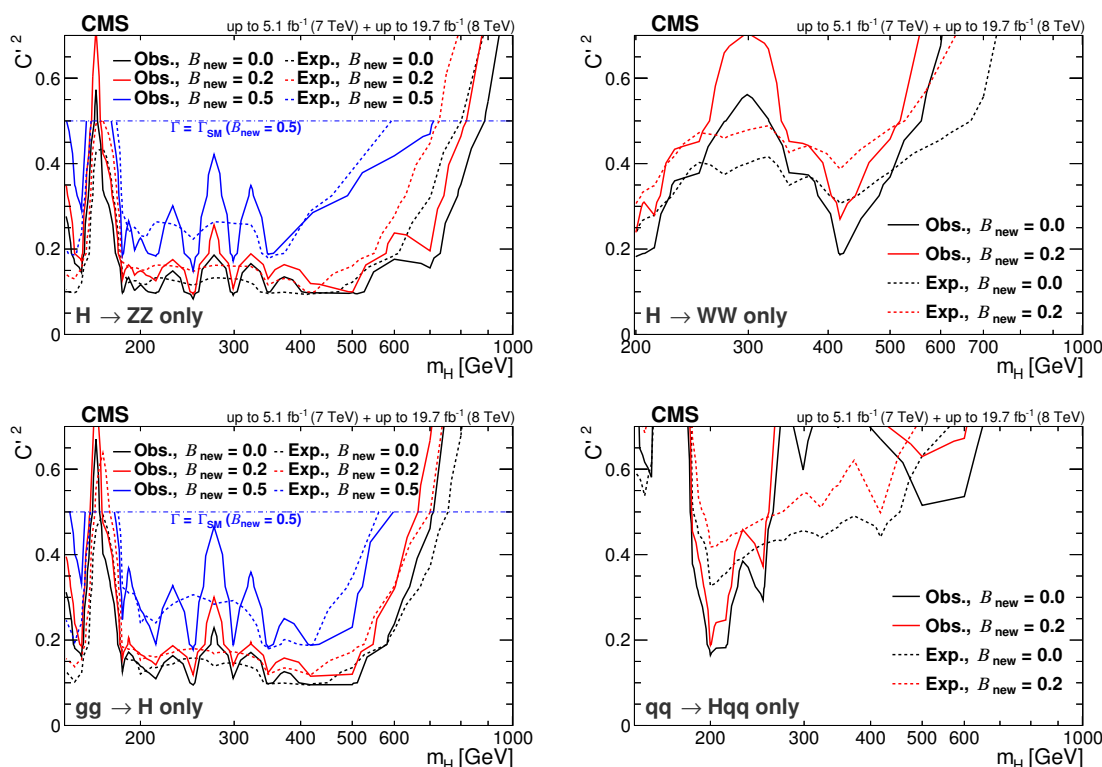
Figure 8. Upper limits at the 95% CL on the EW singlet extension. Upper limits are displayed as a function of the heavy Higgs boson mass and the model parameter C'^2 for different values of $\mathcal{B}_{\text{new}}$. The upper dash-dotted line indicates where, for $\mathcal{B}_{\text{new}} = 0.5$, the variable width of the heavy Higgs boson reaches the width of a SM-like Higgs boson. The lower dash-dotted line displays the indirect limit at 95% CL on C'^2 from the measurement of h(125).

Features in the combined observed limit can be traced to corresponding features in the limits of the individual channels. At lower masses below 400 GeV, there are oscillations in the observed limit due to the high resolution channel, $H \rightarrow ZZ \rightarrow 4\ell$, and the narrow width of the heavy Higgs boson in this mass range. An excess in the combined limit at around 280 GeV is related to a small excess in the channels $H \rightarrow ZZ \rightarrow 4\ell$ and $H \rightarrow WW \rightarrow 2\ell2\nu$. The small excess of observed events seen around 700 GeV in the $H \rightarrow WW \rightarrow \ell\nu J$ merged-jet category is not supported by the other channels and is reduced to less than 0.5σ in the combination. The combined upper limits at the 95% CL on the product of the cross section and branching fractions exclude a Higgs boson with SM-like couplings in the full search range $145 < m_H < 1000$ GeV.

6.2 EW singlet Higgs boson search

We interpret the search results in terms of a heavy Higgs boson in the EW singlet extension of the SM. The parameters of the model are C'^2, the heavy Higgs boson contribution to electroweak symmetry breaking, and $\mathcal{B}_{\text{new}}$, the contribution to the Higgs boson width of non-SM decays, and are defined in section 3. Figure 8 shows the expected and observed upper limits at 95% CL on the singlet scalar cross section with respect to its expected cross section as a function of its mass.

The region above the curves shows the parameter space that is expected to be excluded at 95% CL. We show the exclusion region for various values of $\mathcal{B}_{\text{new}}$. We find a large region of C'^2 versus mass parameters to be excluded for various values of $\mathcal{B}_{\text{new}}$. We also plot the

Figure 9. Upper limits at the 95% CL on the EW singlet extension. Upper limits are displayed as a function of the heavy Higgs boson mass and the model parameter C'^2 for different values of $\mathcal{B}_{\text{new}}$. All considered ZZ decay channels combined (top left). All considered WW decay channels combined (top right). Limits for the ggF production mode only (bottom left). Limits for VBF production only (bottom right). The dash-dotted line in the two left plots indicates where, for $\mathcal{B}_{\text{new}} = 0.5$, the variable width of the heavy Higgs boson reaches the width of a SM-like Higgs boson.

$\mu_{\text{h}(125)} = 1 \pm 0.14$ [85] indirect constraint $C'^2 < 0.28$ at 95% CL for $\mathcal{B}_{\text{new}} = 0$. The upper dash-dotted line shows the cutoff of the allowed region for $\mathcal{B}_{\text{new}} = 0.5$ where the width of the heavy Higgs boson becomes larger than the SM width at that mass hypothesis.

In order to understand the constraints of these results in a model-independent approach, we further subdivide the results into categories. In figure 9 we show the limits in various configurations. At the top of figure 9 are the limits we obtain when we combine the ZZ (top left) and WW (top right) channels separately. Since the ZZ channels are more sensitive in the search for a Higgs boson with SM-like couplings, they better constrain the BSM case as well. The bottom of figure 9 shows the combined 95% CL for all final states but only the ggF or VBF production mechanism for the heavy Higgs boson. In the heavy Higgs boson with SM-like couplings scenario, we assume the ratio of the cross sections for various production mechanisms to be the same as in the SM case.

7 Summary

Combined results are presented from searches for a heavy Higgs boson in H → WW and H → ZZ decay channels, for Higgs boson mass hypotheses in the range $145 < m_{\text{H}} <$

1000 GeV . In the case of a Higgs boson decaying into a pair of W bosons, the fully leptonic ($H \rightarrow WW \rightarrow \ell\nu\ell\nu$) and semileptonic ($H \rightarrow WW \rightarrow \ell\nu qq$) final states are considered in the analysis. For a Higgs boson decaying into two Z bosons, final states containing four charged leptons ($H \rightarrow ZZ \rightarrow 2\ell 2\ell'$), two charged leptons and two quarks ($H \rightarrow ZZ \rightarrow 2\ell 2q$), and two charged leptons and two neutrinos ($H \rightarrow ZZ \rightarrow 2\ell 2\nu$) are considered, where $\ell = e$ or μ and $\ell' = e$, μ, or τ.

The observed data are interpreted both in the context of a heavy Higgs boson with SM-like couplings and decays, as well as a search for a heavy, narrow resonance as an EW singlet partner of the SM Higgs boson at 125 GeV . No significant excess over the expected SM background has been observed and exclusion limits have been set. In the case of the search for a heavy Higgs boson with SM-like couplings and decays, we exclude the existence of such a heavy Higgs boson over the entire search range of $145 < m_H < 1000$ GeV . For the EW singlet partner of the SM Higgs, the parameters of the model are C'^2, the heavy Higgs boson contribution to EW symmetry breaking, and $\mathcal{B}_{\text{new}}$, the contribution to the Higgs boson width of non-SM decays. We find that a large part of the C'^2 versus mass parameter space is excluded for various values of $\mathcal{B}_{\text{new}}$. Additionally, we present limits for the EW singlet model for different production mechanisms, ggF and VBF, and WW and ZZ decay modes separately.

Acknowledgments

References

[1] S.L. Glashow, *Partial-symmetries of weak interactions*, *Nucl. Phys.* **22** (1961) 579.

[2] S. Weinberg, *A Model of Leptons*, *Phys. Rev. Lett.* **19** (1967) 1264 [INSPIRE].

[3] A. Salam, *Weak and electromagnetic interactions*, in *Elementary particle theory: relativistic groups and analyticity*, proceedings of the *Eighth Nobel Symposium*, N. Svartholm ed., Almqvist & Wiksell (1968), p. 367.

[4] F. Englert and R. Brout, *Broken Symmetry and the Mass of Gauge Vector Mesons*, *Phys. Rev. Lett.* **13** (1964) 321 [INSPIRE].

[5] P.W. Higgs, *Broken symmetries, massless particles and gauge fields*, *Phys. Lett.* **12** (1964) 132 [INSPIRE].

[6] P.W. Higgs, *Broken Symmetries and the Masses of Gauge Bosons*, *Phys. Rev. Lett.* **13** (1964) 508 [INSPIRE].

[7] G.S. Guralnik, C.R. Hagen and T.W.B. Kibble, *Global Conservation Laws and Massless Particles*, *Phys. Rev. Lett.* **13** (1964) 585 [INSPIRE].

[8] P.W. Higgs, *Spontaneous Symmetry Breakdown without Massless Bosons*, *Phys. Rev.* **145** (1966) 1156 [INSPIRE].

[9] T.W.B. Kibble, *Symmetry breaking in non-Abelian gauge theories*, *Phys. Rev.* **155** (1967) 1554 [INSPIRE].

[10] ATLAS collaboration, *Observation of a new particle in the search for the Standard Model Higgs boson with the ATLAS detector at the LHC*, *Phys. Lett.* **B 716** (2012) 1 [arXiv:1207.7214] [INSPIRE].

[11] CMS collaboration, *Observation of a new boson at a mass of* 125 *GeV with the CMS experiment at the LHC*, *Phys. Lett.* **B 716** (2012) 30 [arXiv:1207.7235] [INSPIRE].

[12] CMS collaboration, *Observation of a new boson with mass near* 125 *GeV in pp collisions at* $\sqrt{s} = 7$ *and* 8 *TeV*, *JHEP* **06** (2013) 081 [arXiv:1303.4571] [INSPIRE].

[13] ATLAS collaboration, *Measurement of the Higgs boson mass from the* $H \to \gamma\gamma$ *and* $H \to ZZ^* \to 4\ell$ *channels in pp collisions at center-of-mass energies of* 7 *and* 8 *TeV with the ATLAS detector*, *Phys. Rev.* **D 90** (2014) 052004 [arXiv:1406.3827] [INSPIRE].

[14] ATLAS, CMS collaborations, G. Aad et al., *Combined Measurement of the Higgs Boson Mass in pp Collisions at* $\sqrt{s} = 7$ *and* 8 *TeV with the ATLAS and CMS Experiments*, *Phys. Rev. Lett.* **114** (2015) 191803 [arXiv:1503.07589] [INSPIRE].

[15] CMS collaboration, *Search for the standard model Higgs boson produced in association with a top-quark pair in pp collisions at the LHC*, *JHEP* **05** (2013) 145 [arXiv:1303.0763] [INSPIRE].

[16] ATLAS collaboration, *Measurements of Higgs boson production and couplings in diboson final states with the ATLAS detector at the LHC*, *Phys. Lett.* **B 726** (2013) 88 [*Erratum ibid.* **B 734** (2014) 406] [arXiv:1307.1427] [INSPIRE].

[17] CMS collaboration, *Search for the standard model Higgs boson produced in association with a W or a Z boson and decaying to bottom quarks*, *Phys. Rev.* **D 89** (2014) 012003 [arXiv:1310.3687] [INSPIRE].

[18] CMS collaboration, *Measurement of Higgs boson production and properties in the WW decay channel with leptonic final states*, *JHEP* **01** (2014) 096 [arXiv:1312.1129] [INSPIRE].

[19] CMS collaboration, *Measurement of the properties of a Higgs boson in the four-lepton final state*, *Phys. Rev.* **D 89** (2014) 092007 [arXiv:1312.5353] [INSPIRE].

[20] CMS collaboration, *Evidence for the 125 GeV Higgs boson decaying to a pair of τ leptons*, *JHEP* **05** (2014) 104 [arXiv:1401.5041] [INSPIRE].

[21] CMS collaboration, *Observation of the diphoton decay of the Higgs boson and measurement of its properties*, *Eur. Phys. J.* **C 74** (2014) 3076 [arXiv:1407.0558] [INSPIRE].

[22] CMS collaboration, *Search for a Higgs boson decaying into a Z and a photon in pp collisions at $\sqrt{s} = 7$ and $8\,TeV$*, *Phys. Lett.* **B 726** (2013) 587 [arXiv:1307.5515] [INSPIRE].

[23] ATLAS collaboration, *Search for Higgs boson decays to a photon and a Z boson in pp collisions at $\sqrt{s} = 7$ and $8\,TeV$ with the ATLAS detector*, *Phys. Lett.* **B 732** (2014) 8 [arXiv:1402.3051] [INSPIRE].

[24] ATLAS collaboration, *Search for Invisible Decays of a Higgs Boson Produced in Association with a Z Boson in ATLAS*, *Phys. Rev. Lett.* **112** (2014) 201802 [arXiv:1402.3244] [INSPIRE].

[25] CMS collaboration, *Search for invisible decays of Higgs bosons in the vector boson fusion and associated ZH production modes*, *Eur. Phys. J.* **C 74** (2014) 2980 [arXiv:1404.1344] [INSPIRE].

[26] CMS collaboration, *Study of the Mass and Spin-Parity of the Higgs Boson Candidate Via Its Decays to Z Boson Pairs*, *Phys. Rev. Lett.* **110** (2013) 081803 [arXiv:1212.6639] [INSPIRE].

[27] ATLAS collaboration, *Evidence for the spin-0 nature of the Higgs boson using ATLAS data*, *Phys. Lett.* **B 726** (2013) 120 [arXiv:1307.1432] [INSPIRE].

[28] D.A. Dicus and V.S. Mathur, *Upper bounds on the values of masses in unified gauge theories*, *Phys. Rev.* **D 7** (1973) 3111 [INSPIRE].

[29] M.J.G. Veltman, *Second Threshold in Weak Interactions*, *Acta Phys. Polon.* **B 8** (1977) 475 [INSPIRE].

[30] B.W. Lee, C. Quigg and H.B. Thacker, *Weak Interactions at Very High-Energies: The Role of the Higgs Boson Mass*, *Phys. Rev.* **D 16** (1977) 1519 [INSPIRE].

[31] B.W. Lee, C. Quigg and H.B. Thacker, *The Strength of Weak Interactions at Very High-Energies and the Higgs Boson Mass*, *Phys. Rev. Lett.* **38** (1977) 883 [INSPIRE].

[32] G. Passarino, *WW scattering and perturbative unitarity*, *Nucl. Phys.* **B 343** (1990) 31 [INSPIRE].

[33] M.S. Chanowitz and M.K. Gaillard, *The TeV Physics of Strongly Interacting W's and Z's*, *Nucl. Phys.* **B 261** (1985) 379 [INSPIRE].

[34] M.J. Duncan, G.L. Kane and W.W. Repko, *WW Physics at Future Colliders*, *Nucl. Phys.* **B 272** (1986) 517 [INSPIRE].

[35] D.A. Dicus and R. Vega, *WW production from pp collisions*, *Phys. Rev. Lett.* **57** (1986) 1110 [INSPIRE].

[36] J. Bagger et al., *CERN LHC analysis of the strongly interacting WW system: Gold plated modes*, *Phys. Rev.* **D 52** (1995) 3878 [hep-ph/9504426] [INSPIRE].

[37] A. Ballestrero, G. Bevilacqua, D.B. Franzosi and E. Maina, *How well can the LHC distinguish between the SM light Higgs scenario, a composite Higgs and the Higgsless case using VV scattering channels?*, *JHEP* **11** (2009) 126 [arXiv:0909.3838] [INSPIRE].

[38] G.C. Branco, P.M. Ferreira, L. Lavoura, M.N. Rebelo, M. Sher and J.P. Silva, *Theory and phenomenology of two-Higgs-doublet models*, *Phys. Rept.* **516** (2012) 1 [arXiv:1106.0034] [InSPIRE].

[39] N. Craig and S. Thomas, *Exclusive Signals of an Extended Higgs Sector*, *JHEP* **11** (2012) 083 [arXiv:1207.4835] [InSPIRE].

[40] Z. Chacko, H.-S. Goh and R. Harnik, *The Twin Higgs: Natural electroweak breaking from mirror symmetry*, *Phys. Rev. Lett.* **96** (2006) 231802 [hep-ph/0506256] [InSPIRE].

[41] B. Patt and F. Wilczek, *Higgs-field portal into hidden sectors*, hep-ph/0605188 [InSPIRE].

[42] V. Barger, P. Langacker, M. McCaskey, M.J. Ramsey-Musolf and G. Shaughnessy, *LHC Phenomenology of an Extended Standard Model with a Real Scalar Singlet*, *Phys. Rev.* **D 77** (2008) 035005 [arXiv:0706.4311] [InSPIRE].

[43] M. Bowen, Y. Cui and J.D. Wells, *Narrow trans-TeV Higgs bosons and $H \to hh$ decays: Two LHC search paths for a hidden sector Higgs boson*, *JHEP* **03** (2007) 036 [hep-ph/0701035] [InSPIRE].

[44] G. Bhattacharyya, G.C. Branco and S. Nandi, *Universal Doublet-Singlet Higgs Couplings and phenomenology at the CERN Large Hadron Collider*, *Phys. Rev.* **D 77** (2008) 117701 [arXiv:0712.2693] [InSPIRE].

[45] S. Profumo, M.J. Ramsey-Musolf and G. Shaughnessy, *Singlet Higgs phenomenology and the electroweak phase transition*, *JHEP* **08** (2007) 010 [arXiv:0705.2425] [InSPIRE].

[46] S. Dawson and W. Yan, *Hiding the Higgs Boson with Multiple Scalars*, *Phys. Rev.* **D 79** (2009) 095002 [arXiv:0904.2005] [InSPIRE].

[47] S. Bock, R. Lafaye, T. Plehn, M. Rauch, D. Zerwas and P.M. Zerwas, *Measuring Hidden Higgs and Strongly-Interacting Higgs Scenarios*, *Phys. Lett.* **B 694** (2010) 44 [arXiv:1007.2645] [InSPIRE].

[48] S. Baek, P. Ko and W.-I. Park, *Search for the Higgs portal to a singlet fermionic dark matter at the LHC*, *JHEP* **02** (2012) 047 [arXiv:1112.1847] [InSPIRE].

[49] P.J. Fox, D. Tucker-Smith and N. Weiner, *Higgs friends and counterfeits at hadron colliders*, *JHEP* **06** (2011) 127 [arXiv:1104.5450] [InSPIRE].

[50] C. Englert, T. Plehn, D. Zerwas and P.M. Zerwas, *Exploring the Higgs portal*, *Phys. Lett.* **B 703** (2011) 298 [arXiv:1106.3097] [InSPIRE].

[51] C. Englert, J. Jaeckel, E. Re and M. Spannowsky, *Evasive Higgs Maneuvers at the LHC*, *Phys. Rev.* **D 85** (2012) 035008 [arXiv:1111.1719] [InSPIRE].

[52] B. Batell, S. Gori and L.-T. Wang, *Exploring the Higgs Portal with $10\,fb^{-1}$ at the LHC*, *JHEP* **06** (2012) 172 [arXiv:1112.5180] [InSPIRE].

[53] C. Englert, T. Plehn, M. Rauch, D. Zerwas and P.M. Zerwas, *LHC: Standard Higgs and Hidden Higgs*, *Phys. Lett.* **B 707** (2012) 512 [arXiv:1112.3007] [InSPIRE].

[54] R.S. Gupta and J.D. Wells, *Higgs boson search significance deformations due to mixed-in scalars*, *Phys. Lett.* **B 710** (2012) 154 [arXiv:1110.0824] [InSPIRE].

[55] M.J. Dolan, C. Englert and M. Spannowsky, *New Physics in LHC Higgs boson pair production*, *Phys. Rev.* **D 87** (2013) 055002 [arXiv:1210.8166] [InSPIRE].

[56] D. Bertolini and M. McCullough, *The Social Higgs*, *JHEP* **12** (2012) 118 [arXiv:1207.4209] [InSPIRE].

[57] B. Batell, D. McKeen and M. Pospelov, *Singlet Neighbors of the Higgs Boson*, *JHEP* **10** (2012) 104 [`arXiv:1207.6252`] [ɪɴSPIRE].

[58] S. Choi, S. Jung and P. Ko, *Implications of LHC data on* 125 *GeV Higgs-like boson for the Standard Model and its various extensions*, *JHEP* **10** (2013) 225 [`arXiv:1307.3948`] [ɪɴSPIRE].

[59] T. Hambye and A. Strumia, *Dynamical generation of the weak and Dark Matter scale*, *Phys. Rev.* **D 88** (2013) 055022 [`arXiv:1306.2329`] [ɪɴSPIRE].

[60] N. Craig, H.K. Lou, M. McCullough and A. Thalapillil, *The Higgs Portal Above Threshold*, `arXiv:1412.0258` [ɪɴSPIRE].

[61] D. Curtin, P. Meade and C.-T. Yu, *Testing Electroweak Baryogenesis with Future Colliders*, *JHEP* **11** (2014) 127 [`arXiv:1409.0005`] [ɪɴSPIRE].

[62] D. López-Val and T. Robens, Δr *and the* W-*boson mass in the singlet extension of the standard model*, *Phys. Rev.* **D 90** (2014) 114018 [`arXiv:1406.1043`] [ɪɴSPIRE].

[63] T. Robens and T. Stefaniak, *Status of the Higgs Singlet Extension of the Standard Model after LHC Run 1*, *Eur. Phys. J.* **C 75** (2015) 104 [`arXiv:1501.02234`] [ɪɴSPIRE].

[64] CMS collaboration, *Search for a standard-model-like Higgs boson with a mass in the range* 145 *to* 1000 *GeV at the LHC*, *Eur. Phys. J.* **C 73** (2013) 2469 [`arXiv:1304.0213`] [ɪɴSPIRE].

[65] CMS collaboration, *The CMS experiment at the CERN LHC*, 2008 *JINST* **3** S08004 [ɪɴSPIRE].

[66] E. Bagnaschi, G. Degrassi, P. Slavich and A. Vicini, *Higgs production via gluon fusion in the POWHEG approach in the SM and in the MSSM*, *JHEP* **02** (2012) 088 [`arXiv:1111.2854`] [ɪɴSPIRE].

[67] P. Nason, *A New method for combining NLO QCD with shower Monte Carlo algorithms*, *JHEP* **11** (2004) 040 [`hep-ph/0409146`] [ɪɴSPIRE].

[68] S. Frixione, P. Nason and C. Oleari, *Matching NLO QCD computations with Parton Shower simulations: the POWHEG method*, *JHEP* **11** (2007) 070 [`arXiv:0709.2092`] [ɪɴSPIRE].

[69] S. Alioli, P. Nason, C. Oleari and E. Re, *A general framework for implementing NLO calculations in shower Monte Carlo programs: the POWHEG BOX*, *JHEP* **06** (2010) 043 [`arXiv:1002.2581`] [ɪɴSPIRE].

[70] P. Nason and C. Oleari, *NLO Higgs boson production via vector-boson fusion matched with shower in POWHEG*, *JHEP* **02** (2010) 037 [`arXiv:0911.5299`] [ɪɴSPIRE].

[71] Y. Gao, A.V. Gritsan, Z. Guo, K. Melnikov, M. Schulze and N.V. Tran, *Spin determination of single-produced resonances at hadron colliders*, *Phys. Rev.* **D 81** (2010) 075022 [`arXiv:1001.3396`] [ɪɴSPIRE].

[72] T. Sjöstrand, S. Mrenna and P.Z. Skands, *PYTHIA* 6.4 *Physics and Manual*, *JHEP* **05** (2006) 026 [`hep-ph/0603175`] [ɪɴSPIRE].

[73] LHC Higgs Cross Section Working Group collaboration, J.R. Andersen et al., *Handbook of LHC Higgs Cross Sections: 3. Higgs Properties*, `arXiv:1307.1347` [CERN-2013-004] [ɪɴSPIRE].

[74] G. Passarino, C. Sturm and S. Uccirati, *Higgs Pseudo-Observables, Second Riemann Sheet and All That*, *Nucl. Phys.* **B 834** (2010) 77 [`arXiv:1001.3360`] [ɪɴSPIRE].

[75] S. Goria, G. Passarino and D. Rosco, *The Higgs Boson Lineshape*, *Nucl. Phys.* **B 864** (2012) 530 [arXiv:1112.5517] [INSPIRE].

[76] N. Kauer and G. Passarino, *Inadequacy of zero-width approximation for a light Higgs boson signal*, *JHEP* **08** (2012) 116 [arXiv:1206.4803] [INSPIRE].

[77] J. Alwall et al., *MadGraph/MadEvent v4: The New Web Generation*, *JHEP* **09** (2007) 028 [arXiv:0706.2334] [INSPIRE].

[78] T. Binoth, M. Ciccolini, N. Kauer and M. Krämer, *Gluon-induced W-boson pair production at the LHC*, *JHEP* **12** (2006) 046 [hep-ph/0611170] [INSPIRE].

[79] T. Binoth, N. Kauer and P. Mertsch, *Gluon-induced QCD corrections to $pp \to ZZ \to \ell\bar{\ell}\ell'\bar{\ell}'$*, in proceedings of the *XVI International Workshop on Deep-Inelastic Scattering and Related Subjects (DIS'07)* 2008 [arXiv:0807.0024] [INSPIRE].

[80] H.-L. Lai et al., *Uncertainty induced by QCD coupling in the CTEQ global analysis of parton distributions*, *Phys. Rev.* **D 82** (2010) 054021 [arXiv:1004.4624] [INSPIRE].

[81] H.-L. Lai et al., *New parton distributions for collider physics*, *Phys. Rev.* **D 82** (2010) 074024 [arXiv:1007.2241] [INSPIRE].

[82] S. Jadach, Z. Wąs, R. Decker and J.H. Kühn, *The τ decay library TAUOLA: Version* 2.4, *Comput. Phys. Commun.* **76** (1993) 361 [INSPIRE].

[83] GEANT4 collaboration, S. Agostinelli et al., *GEANT4: A Simulation toolkit*, *Nucl. Instrum. Meth.* **A 506** (2003) 250 [INSPIRE].

[84] CMS collaboration, *Measurement of the Underlying Event Activity at the LHC with $\sqrt{s} = 7\, TeV$ and Comparison with $\sqrt{s} = 0.9\, TeV$*, *JHEP* **09** (2011) 109 [arXiv:1107.0330] [INSPIRE].

[85] CMS collaboration, *Precise determination of the mass of the Higgs boson and tests of compatibility of its couplings with the standard model predictions using proton collisions at 7 and 8 TeV*, *Eur. Phys. J.* **C 75** (2015) 212 [arXiv:1412.8662] [INSPIRE].

[86] J.M. Campbell and R.K. Ellis, *MCFM for the Tevatron and the LHC*, *Nucl. Phys. Proc. Suppl.* **205-206** (2010) 10 [arXiv:1007.3492] [INSPIRE].

[87] A. Ballestrero, A. Belhouari, G. Bevilacqua, V. Kashkan and E. Maina, *PHANTOM: A Monte Carlo event generator for six parton final states at high energy colliders*, *Comput. Phys. Commun.* **180** (2009) 401 [arXiv:0801.3359] [INSPIRE].

[88] C. Englert, Y. Soreq and M. Spannowsky, *Off-Shell Higgs Coupling Measurements in BSM scenarios*, *JHEP* **05** (2015) 145 [arXiv:1410.5440] [INSPIRE].

[89] E. Maina, *Interference effects in Heavy Higgs production via gluon fusion in the Singlet Extension of the Standard Model*, *JHEP* **06** (2015) 004 [arXiv:1501.02139] [INSPIRE].

[90] CMS collaboration, *Particle-Flow Event Reconstruction in CMS and Performance for Jets, Taus and MET*, CMS-PAS-PFT-09-001.

[91] CMS collaboration, *Missing transverse energy performance of the CMS detector*, 2011 *JINST* **6** P09001 [arXiv:1106.5048] [INSPIRE].

[92] CMS collaboration, *Performance of CMS muon reconstruction in pp collision events at $\sqrt{s} = 7\, TeV$*, 2012 *JINST* **7** P10002 [arXiv:1206.4071] [INSPIRE].

[93] CMS collaboration, *Description and performance of track and primary-vertex reconstruction with the CMS tracker*, 2014 *JINST* **9** P10009 [arXiv:1405.6569] [INSPIRE].

[94] CMS collaboration, *Performance of electron reconstruction and selection with the CMS detector in proton-proton collisions at $\sqrt{s} = 8\,TeV$*, 2015 *JINST* **10** P06005 [arXiv:1502.02701] [INSPIRE].

[95] CMS collaboration, *Performance of τ-lepton reconstruction and identification in CMS*, 2012 *JINST* **7** P01001 [arXiv:1109.6034] [INSPIRE].

[96] M. Cacciari and G.P. Salam, *Pileup subtraction using jet areas*, *Phys. Lett.* **B 659** (2008) 119 [arXiv:0707.1378] [INSPIRE].

[97] CMS collaboration, *Determination of Jet Energy Calibration and Transverse Momentum Resolution in CMS*, 2011 *JINST* **6** P11002 [arXiv:1107.4277] [INSPIRE].

[98] M. Cacciari, G.P. Salam and G. Soyez, *The Anti-k_t jet clustering algorithm*, *JHEP* **04** (2008) 063 [arXiv:0802.1189] [INSPIRE].

[99] M. Cacciari, G.P. Salam and G. Soyez, *FastJet User Manual*, *Eur. Phys. J.* **C 72** (2012) 1896 [arXiv:1111.6097] [INSPIRE].

[100] Y.L. Dokshitzer, G.D. Leder, S. Moretti and B.R. Webber, *Better jet clustering algorithms*, *JHEP* **08** (1997) 001 [hep-ph/9707323] [INSPIRE].

[101] M. Cacciari, G.P. Salam and G. Soyez, *The Catchment Area of Jets*, *JHEP* **04** (2008) 005 [arXiv:0802.1188] [INSPIRE].

[102] CMS collaboration, *Pileup Jet Identification*, CMS-PAS-JME-13-005.

[103] CMS collaboration, *Identification techniques for highly boosted W bosons that decay into hadrons*, *JHEP* **12** (2014) 017 [arXiv:1410.4227] [INSPIRE].

[104] J. Thaler and K. Van Tilburg, *Identifying Boosted Objects with N-subjettiness*, *JHEP* **03** (2011) 015 [arXiv:1011.2268] [INSPIRE].

[105] CMS collaboration, *Identification of b-quark jets with the CMS experiment*, 2013 *JINST* **8** P04013 [arXiv:1211.4462] [INSPIRE].

[106] CMS collaboration, *CMS MET Performance in Events Containing Electroweak Bosons from pp Collisions at $\sqrt{s} = 7\,TeV$*, CMS-PAS-JME-10-005.

[107] M. Ciccolini, A. Denner and S. Dittmaier, *Strong and electroweak corrections to the production of Higgs + 2 jets via weak interactions at the LHC*, *Phys. Rev. Lett.* **99** (2007) 161803 [arXiv:0707.0381] [INSPIRE].

[108] M. Ciccolini, A. Denner and S. Dittmaier, *Electroweak and QCD corrections to Higgs production via vector-boson fusion at the LHC*, *Phys. Rev.* **D 77** (2008) 013002 [arXiv:0710.4749] [INSPIRE].

[109] K. Arnold et al., *VBFNLO: A Parton level Monte Carlo for processes with electroweak bosons*, *Comput. Phys. Commun.* **180** (2009) 1661 [arXiv:0811.4559] [INSPIRE].

[110] R.N. Cahn, S.D. Ellis, R. Kleiss and W.J. Stirling, *Transverse Momentum Signatures for Heavy Higgs Bosons*, *Phys. Rev.* **D 35** (1987) 1626 [INSPIRE].

[111] S. Alekhin et al., *The PDF4LHC Working Group Interim Report*, arXiv:1101.0536 [INSPIRE].

[112] M. Botje et al., *The PDF4LHC Working Group Interim Recommendations*, arXiv:1101.0538 [INSPIRE].

[113] A.D. Martin, W.J. Stirling, R.S. Thorne and G. Watt, *Parton distributions for the LHC*, *Eur. Phys. J.* **C 63** (2009) 189 [arXiv:0901.0002] [INSPIRE].

[114] R.D. Ball, V. Bertone, F. Cerutti, L. Del Debbio, S. Forte, A. Guffanti et al., *Impact of Heavy Quark Masses on Parton Distributions and LHC Phenomenology*, *Nucl. Phys.* **B 849** (2011) 296 [arXiv:1101.1300] [inSPIRE].

[115] B.A. Dobrescu and J.D. Lykken, *Semileptonic decays of the standard Higgs boson*, *JHEP* **04** (2010) 083 [arXiv:0912.3543] [inSPIRE].

[116] CMS collaboration, *Search for the standard model Higgs boson in the H to ZZ to ℓℓττ decay channel in pp collisions at $\sqrt{s} = 7$ TeV*, *JHEP* **03** (2012) 081 [arXiv:1202.3617] [inSPIRE].

[117] I. Anderson et al., *Constraining anomalous HVV interactions at proton and lepton colliders*, *Phys. Rev.* **D 89** (2014) 035007 [arXiv:1309.4819] [inSPIRE].

[118] CMS collaboration, *Search for the standard model Higgs boson in the H to ZZ to 2 ℓ2ν channel in pp collisions at $\sqrt{s} = 7$ TeV*, *JHEP* **03** (2012) 040 [arXiv:1202.3478] [inSPIRE].

[119] CMS collaboration, *Search for a Higgs boson in the decay channel* $H \to ZZ^* \to q\bar{q}\ell^+\ell^-$ *in pp collisions at $\sqrt{s} = 7$ TeV*, *JHEP* **04** (2012) 036 [arXiv:1202.1416] [inSPIRE].

[120] ATLAS, CMS, Higgs Combination Group collaborations, *Procedure for the LHC Higgs boson search combination in Summer 2011*, ATL-PHYS-PUB 2011-11, CMS-NOTE-2011-005.

[121] CMS collaboration, *Combined results of searches for the standard model Higgs boson in pp collisions at $\sqrt{s} = 7$ TeV*, *Phys. Lett.* **B 710** (2012) 26 [arXiv:1202.1488] [inSPIRE].

[122] A.L. Read, *Modified frequentist analysis of search results (the CL_s method)*, CERN-OPEN-2000-205 (2000).

[123] T. Junk, *Confidence level computation for combining searches with small statistics*, *Nucl. Instrum. Meth.* **A 434** (1999) 435 [hep-ex/9902006] [inSPIRE].

The CMS collaboration

Yerevan Physics Institute, Yerevan, Armenia

V. Khachatryan, A.M. Sirunyan, A. Tumasyan

Institut für Hochenergiephysik der OeAW, Wien, Austria

W. Adam, E. Asilar, T. Bergauer, J. Brandstetter, E. Brondolin, M. Dragicevic, J. Erö, M. Flechl, M. Friedl, R. Frühwirth[1], V.M. Ghete, C. Hartl, N. Hörmann, J. Hrubec, M. Jeitler[1], V. Knünz, A. König, M. Krammer[1], I. Krätschmer, D. Liko, T. Matsushita, I. Mikulec, D. Rabady[2], B. Rahbaran, H. Rohringer, J. Schieck[1], R. Schöfbeck, J. Strauss, W. Treberer-Treberspurg, W. Waltenberger, C.-E. Wulz[1]

National Centre for Particle and High Energy Physics, Minsk, Belarus

V. Mossolov, N. Shumeiko, J. Suarez Gonzalez

Universiteit Antwerpen, Antwerpen, Belgium

S. Alderweireldt, T. Cornelis, E.A. De Wolf, X. Janssen, A. Knutsson, J. Lauwers, S. Luyckx, S. Ochesanu, R. Rougny, M. Van De Klundert, H. Van Haevermaet, P. Van Mechelen, N. Van Remortel, A. Van Spilbeeck

Vrije Universiteit Brussel, Brussel, Belgium

S. Abu Zeid, F. Blekman, J. D'Hondt, N. Daci, I. De Bruyn, K. Deroover, N. Heracleous, J. Keaveney, S. Lowette, L. Moreels, A. Olbrechts, Q. Python, D. Strom, S. Tavernier, W. Van Doninck, P. Van Mulders, G.P. Van Onsem, I. Van Parijs

Université Libre de Bruxelles, Bruxelles, Belgium

P. Barria, C. Caillol, B. Clerbaux, G. De Lentdecker, H. Delannoy, D. Dobur, G. Fasanella, L. Favart, A.P.R. Gay, A. Grebenyuk, A. Léonard, A. Mohammadi, L. Perniè, A. Randleconde, T. Reis, T. Seva, L. Thomas, C. Vander Velde, P. Vanlaer, J. Wang, F. Zenoni, F. Zhang[3]

Ghent University, Ghent, Belgium

K. Beernaert, L. Benucci, A. Cimmino, S. Crucy, A. Fagot, G. Garcia, M. Gul, J. Mccartin, A.A. Ocampo Rios, D. Poyraz, D. Ryckbosch, S. Salva Diblen, M. Sigamani, N. Strobbe, M. Tytgat, W. Van Driessche, E. Yazgan, N. Zaganidis

Université Catholique de Louvain, Louvain-la-Neuve, Belgium

S. Basegmez, C. Beluffi[4], O. Bondu, G. Bruno, R. Castello, A. Caudron, L. Ceard, G.G. Da Silveira, C. Delaere, T. du Pree, D. Favart, L. Forthomme, A. Giammanco[5], J. Hollar, A. Jafari, P. Jez, M. Komm, V. Lemaitre, A. Mertens, C. Nuttens, L. Perrini, A. Pin, K. Piotrzkowski, A. Popov[6], L. Quertenmont, M. Selvaggi, M. Vidal Marono

Université de Mons, Mons, Belgium

N. Beliy, T. Caebergs, G.H. Hammad

Centro Brasileiro de Pesquisas Fisicas, Rio de Janeiro, Brazil

W.L. Aldá Júnior, G.A. Alves, L. Brito, M. Correa Martins Junior, T. Dos Reis Martins, C. Hensel, C. Mora Herrera, A. Moraes, M.E. Pol, P. Rebello Teles

Universidade do Estado do Rio de Janeiro, Rio de Janeiro, Brazil

E. Belchior Batista Das Chagas, W. Carvalho, J. Chinellato[7], A. Custódio, E.M. Da Costa, D. De Jesus Damiao, C. De Oliveira Martins, S. Fonseca De Souza, L.M. Huertas Guativa, H. Malbouisson, D. Matos Figueiredo, L. Mundim, H. Nogima, W.L. Prado Da Silva, J. Santaolalla, A. Santoro, A. Sznajder, E.J. Tonelli Manganote[7], A. Vilela Pereira

Universidade Estadual Paulista [a], Universidade Federal do ABC [b], São Paulo, Brazil

S. Ahuja, C.A. Bernardes[b], S. Dogra[a], T.R. Fernandez Perez Tomei[a], E.M. Gregores[b], P.G. Mercadante[b], C.S. Moon[a,8], S.F. Novaes[a], Sandra S. Padula[a], D. Romero Abad, J.C. Ruiz Vargas

Institute for Nuclear Research and Nuclear Energy, Sofia, Bulgaria

A. Aleksandrov, V. Genchev[2], R. Hadjiiska, P. Iaydjiev, A. Marinov, S. Piperov, M. Rodozov, S. Stoykova, G. Sultanov, M. Vutova

University of Sofia, Sofia, Bulgaria

A. Dimitrov, I. Glushkov, L. Litov, B. Pavlov, P. Petkov

Institute of High Energy Physics, Beijing, China

M. Ahmad, J.G. Bian, G.M. Chen, H.S. Chen, M. Chen, T. Cheng, R. Du, C.H. Jiang, R. Plestina[9], F. Romeo, S.M. Shaheen, J. Tao, C. Wang, Z. Wang, H. Zhang

State Key Laboratory of Nuclear Physics and Technology, Peking University, Beijing, China

C. Asawatangtrakuldee, Y. Ban, Q. Li, S. Liu, Y. Mao, S.J. Qian, D. Wang, Z. Xu, W. Zou

Universidad de Los Andes, Bogota, Colombia

C. Avila, A. Cabrera, L.F. Chaparro Sierra, C. Florez, J.P. Gomez, B. Gomez Moreno, J.C. Sanabria

University of Split, Faculty of Electrical Engineering, Mechanical Engineering and Naval Architecture, Split, Croatia

N. Godinovic, D. Lelas, D. Polic, I. Puljak

University of Split, Faculty of Science, Split, Croatia

Z. Antunovic, M. Kovac

Institute Rudjer Boskovic, Zagreb, Croatia

V. Brigljevic, K. Kadija, J. Luetic, L. Sudic

University of Cyprus, Nicosia, Cyprus

A. Attikis, G. Mavromanolakis, J. Mousa, C. Nicolaou, F. Ptochos, P.A. Razis, H. Rykaczewski

Charles University, Prague, Czech Republic

M. Bodlak, M. Finger[10], M. Finger Jr.[10]

Academy of Scientific Research and Technology of the Arab Republic of Egypt, Egyptian Network of High Energy Physics, Cairo, Egypt

A. Ali[11,12], R. Aly[13], S. Aly[13], Y. Assran[14], A. Ellithi Kamel[15], A. Lotfy[16], M.A. Mahmoud[16], R. Masod[11], A. Radi[12,11]

National Institute of Chemical Physics and Biophysics, Tallinn, Estonia

B. Calpas, M. Kadastik, M. Murumaa, M. Raidal, A. Tiko, C. Veelken

Department of Physics, University of Helsinki, Helsinki, Finland

P. Eerola, M. Voutilainen

Helsinki Institute of Physics, Helsinki, Finland

J. Härkönen, V. Karimäki, R. Kinnunen, T. Lampén, K. Lassila-Perini, S. Lehti, T. Lindén, P. Luukka, T. Mäenpää, J. Pekkanen, T. Peltola, E. Tuominen, J. Tuominiemi, E. Tuovinen, L. Wendland

Lappeenranta University of Technology, Lappeenranta, Finland

J. Talvitie, T. Tuuva

DSM/IRFU, CEA/Saclay, Gif-sur-Yvette, France

M. Besancon, F. Couderc, M. Dejardin, D. Denegri, B. Fabbro, J.L. Faure, C. Favaro, F. Ferri, S. Ganjour, A. Givernaud, P. Gras, G. Hamel de Monchenault, P. Jarry, E. Locci, M. Machet, J. Malcles, J. Rander, A. Rosowsky, M. Titov, A. Zghiche

Laboratoire Leprince-Ringuet, Ecole Polytechnique, IN2P3-CNRS, Palaiseau, France

S. Baffioni, F. Beaudette, P. Busson, L. Cadamuro, E. Chapon, C. Charlot, T. Dahms, O. Davignon, N. Filipovic, A. Florent, R. Granier de Cassagnac, S. Lisniak, L. Mastrolorenzo, P. Miné, I.N. Naranjo, M. Nguyen, C. Ochando, G. Ortona, P. Paganini, S. Regnard, R. Salerno, J.B. Sauvan, Y. Sirois, T. Strebler, Y. Yilmaz, A. Zabi

Institut Pluridisciplinaire Hubert Curien, Université de Strasbourg, Université de Haute Alsace Mulhouse, CNRS/IN2P3, Strasbourg, France

J.-L. Agram[17], J. Andrea, A. Aubin, D. Bloch, J.-M. Brom, M. Buttignol, E.C. Chabert, N. Chanon, C. Collard, E. Conte[17], J.-C. Fontaine[17], D. Gelé, U. Goerlach, C. Goetzmann, A.-C. Le Bihan, J.A. Merlin[2], K. Skovpen, P. Van Hove

Centre de Calcul de l'Institut National de Physique Nucleaire et de Physique des Particules, CNRS/IN2P3, Villeurbanne, France

S. Gadrat

Université de Lyon, Université Claude Bernard Lyon 1, CNRS-IN2P3, Institut de Physique Nucléaire de Lyon, Villeurbanne, France

S. Beauceron, N. Beaupere, C. Bernet[9], G. Boudoul[2], E. Bouvier, S. Brochet, C.A. Carrillo Montoya, J. Chasserat, R. Chierici, D. Contardo, B. Courbon, P. Depasse, H. El Mamouni, J. Fan, J. Fay, S. Gascon, M. Gouzevitch, B. Ille, I.B. Laktineh, M. Lethuillier, L. Mirabito, A.L. Pequegnot, S. Perries, J.D. Ruiz Alvarez, D. Sabes, L. Sgandurra, V. Sordini, M. Vander Donckt, P. Verdier, S. Viret, H. Xiao

Institute of High Energy Physics and Informatization, Tbilisi State University, Tbilisi, Georgia

Z. Tsamalaidze[10]

RWTH Aachen University, I. Physikalisches Institut, Aachen, Germany

C. Autermann, S. Beranek, M. Edelhoff, L. Feld, A. Heister, M.K. Kiesel, K. Klein, M. Lipinski, A. Ostapchuk, M. Preuten, F. Raupach, J. Sammet, S. Schael, J.F. Schulte, T. Verlage, H. Weber, B. Wittmer, V. Zhukov[6]

RWTH Aachen University, III. Physikalisches Institut A, Aachen, Germany

M. Ata, M. Brodski, E. Dietz-Laursonn, D. Duchardt, M. Endres, M. Erdmann, S. Erdweg, T. Esch, R. Fischer, A. Güth, T. Hebbeker, C. Heidemann, K. Hoepfner, D. Klingebiel, S. Knutzen, P. Kreuzer, M. Merschmeyer, A. Meyer, P. Millet, M. Olschewski, K. Padeken, P. Papacz, T. Pook, M. Radziej, H. Reithler, M. Rieger, F. Scheuch, L. Sonnenschein, D. Teyssier, S. Thüer

RWTH Aachen University, III. Physikalisches Institut B, Aachen, Germany

V. Cherepanov, Y. Erdogan, G. Flügge, H. Geenen, M. Geisler, W. Haj Ahmad, F. Hoehle, B. Kargoll, T. Kress, Y. Kuessel, A. Künsken, J. Lingemann[2], A. Nehrkorn, A. Nowack, I.M. Nugent, C. Pistone, O. Pooth, A. Stahl

Deutsches Elektronen-Synchrotron, Hamburg, Germany

M. Aldaya Martin, I. Asin, N. Bartosik, O. Behnke, U. Behrens, A.J. Bell, K. Borras, A. Burgmeier, A. Cakir, L. Calligaris, A. Campbell, S. Choudhury, F. Costanza, C. Diez Pardos, G. Dolinska, S. Dooling, T. Dorland, G. Eckerlin, D. Eckstein, T. Eichhorn, G. Flucke, E. Gallo, J. Garay Garcia, A. Geiser, A. Gizhko, P. Gunnellini, J. Hauk, M. Hempel[18], H. Jung, A. Kalogeropoulos, O. Karacheban[18], M. Kasemann, P. Katsas, J. Kieseler, C. Kleinwort, I. Korol, W. Lange, J. Leonard, K. Lipka, A. Lobanov, W. Lohmann[18], R. Mankel, I. Marfin[18], I.-A. Melzer-Pellmann, A.B. Meyer, G. Mittag, J. Mnich, A. Mussgiller, S. Naumann-Emme, A. Nayak, E. Ntomari, H. Perrey, D. Pitzl, R. Placakyte, A. Raspereza, P.M. Ribeiro Cipriano, B. Roland, M.Ö. Sahin, J. Salfeld-Nebgen, P. Saxena, T. Schoerner-Sadenius, M. Schröder, C. Seitz, S. Spannagel, K.D. Trippkewitz, C. Wissing

University of Hamburg, Hamburg, Germany

V. Blobel, M. Centis Vignali, A.R. Draeger, J. Erfle, E. Garutti, K. Goebel, D. Gonzalez, M. Görner, J. Haller, M. Hoffmann, R.S. Höing, A. Junkes, R. Klanner, R. Kogler, T. Lapsien, T. Lenz, I. Marchesini, D. Marconi, D. Nowatschin, J. Ott, F. Pantaleo[2], T. Peiffer, A. Perieanu, N. Pietsch, J. Poehlsen, D. Rathjens, C. Sander, H. Schettler, P. Schleper, E. Schlieckau, A. Schmidt, M. Seidel, V. Sola, H. Stadie, G. Steinbrück, H. Tholen, D. Troendle, E. Usai, L. Vanelderen, A. Vanhoefer

Institut für Experimentelle Kernphysik, Karlsruhe, Germany

M. Akbiyik, C. Barth, C. Baus, J. Berger, C. Böser, E. Butz, T. Chwalek, F. Colombo, W. De Boer, A. Descroix, A. Dierlamm, M. Feindt, F. Frensch, M. Giffels, A. Gilbert, F. Hartmann[2], U. Husemann, F. Kassel[2], I. Katkov[6], A. Kornmayer[2], P. Lobelle Pardo,

M.U. Mozer, T. Müller, Th. Müller, M. Plagge, G. Quast, K. Rabbertz, S. Röcker, F. Roscher, H.J. Simonis, F.M. Stober, R. Ulrich, J. Wagner-Kuhr, S. Wayand, T. Weiler, C. Wöhrmann, R. Wolf

Institute of Nuclear and Particle Physics (INPP), NCSR Demokritos, Aghia Paraskevi, Greece

G. Anagnostou, G. Daskalakis, T. Geralis, V.A. Giakoumopoulou, A. Kyriakis, D. Loukas, A. Markou, A. Psallidas, I. Topsis-Giotis

University of Athens, Athens, Greece

A. Agapitos, S. Kesisoglou, A. Panagiotou, N. Saoulidou, E. Tziaferi

University of Ioánnina, Ioánnina, Greece

I. Evangelou, G. Flouris, C. Foudas, P. Kokkas, N. Loukas, N. Manthos, I. Papadopoulos, E. Paradas, J. Strologas

Wigner Research Centre for Physics, Budapest, Hungary

G. Bencze, C. Hajdu, A. Hazi, P. Hidas, D. Horvath[19], F. Sikler, V. Veszpremi, G. Vesztergombi[20], A.J. Zsigmond

Institute of Nuclear Research ATOMKI, Debrecen, Hungary

N. Beni, S. Czellar, J. Karancsi[21], J. Molnar, Z. Szillasi

University of Debrecen, Debrecen, Hungary

M. Bartók[22], A. Makovec, P. Raics, Z.L. Trocsanyi, B. Ujvari

National Institute of Science Education and Research, Bhubaneswar, India

P. Mal, K. Mandal, N. Sahoo, S.K. Swain

Panjab University, Chandigarh, India

S. Bansal, S.B. Beri, V. Bhatnagar, R. Chawla, R. Gupta, U.Bhawandeep, A.K. Kalsi, A. Kaur, M. Kaur, R. Kumar, A. Mehta, M. Mittal, N. Nishu, J.B. Singh, G. Walia

University of Delhi, Delhi, India

Ashok Kumar, Arun Kumar, A. Bhardwaj, B.C. Choudhary, R.B. Garg, A. Kumar, S. Malhotra, M. Naimuddin, K. Ranjan, R. Sharma, V. Sharma

Saha Institute of Nuclear Physics, Kolkata, India

S. Banerjee, S. Bhattacharya, K. Chatterjee, S. Dey, S. Dutta, Sa. Jain, Sh. Jain, R. Khurana, N. Majumdar, A. Modak, K. Mondal, S. Mukherjee, S. Mukhopadhyay, A. Roy, D. Roy, S. Roy Chowdhury, S. Sarkar, M. Sharan

Bhabha Atomic Research Centre, Mumbai, India

A. Abdulsalam, R. Chudasama, D. Dutta, V. Jha, V. Kumar, A.K. Mohanty[2], L.M. Pant, P. Shukla, A. Topkar

Tata Institute of Fundamental Research, Mumbai, India

T. Aziz, S. Banerjee, S. Bhowmik[23], R.M. Chatterjee, R.K. Dewanjee, S. Dugad, S. Ganguly, S. Ghosh, M. Guchait, A. Gurtu[24], G. Kole, S. Kumar, B. Mahakud, M. Maity[23],

G. Majumder, K. Mazumdar, S. Mitra, G.B. Mohanty, B. Parida, T. Sarkar[23], K. Sudhakar, N. Sur, B. Sutar, N. Wickramage[25]

Indian Institute of Science Education and Research (IISER), Pune, India

S. Sharma

Institute for Research in Fundamental Sciences (IPM), Tehran, Iran

H. Bakhshiansohi, H. Behnamian, S.M. Etesami[26], A. Fahim[27], R. Goldouzian, M. Khakzad, M. Mohammadi Najafabadi, M. Naseri, S. Paktinat Mehdiabadi, F. Rezaei Hosseinabadi, B. Safarzadeh[28], M. Zeinali

University College Dublin, Dublin, Ireland

M. Felcini, M. Grunewald

INFN Sezione di Bari [a], Università di Bari [b], Politecnico di Bari [c], Bari, Italy

M. Abbrescia[a,b], C. Calabria[a,b], C. Caputo[a,b], S.S. Chhibra[a,b], A. Colaleo[a], D. Creanza[a,c], L. Cristella[a,b], N. De Filippis[a,c], M. De Palma[a,b], L. Fiore[a], G. Iaselli[a,c], G. Maggi[a,c], M. Maggi[a], G. Miniello[a,b], S. My[a,c], S. Nuzzo[a,b], A. Pompili[a,b], G. Pugliese[a,c], R. Radogna[a,b,2], A. Ranieri[a], G. Selvaggi[a,b], A. Sharma[a], L. Silvestris[a,2], R. Venditti[a,b], P. Verwilligen[a]

INFN Sezione di Bologna [a], Università di Bologna [b], Bologna, Italy

G. Abbiendi[a], C. Battilana, A.C. Benvenuti[a], D. Bonacorsi[a,b], S. Braibant-Giacomelli[a,b], L. Brigliadori[a,b], R. Campanini[a,b], P. Capiluppi[a,b], A. Castro[a,b], F.R. Cavallo[a], G. Codispoti[a,b], M. Cuffiani[a,b], G.M. Dallavalle[a], F. Fabbri[a], A. Fanfani[a,b], D. Fasanella[a,b], P. Giacomelli[a], C. Grandi[a], L. Guiducci[a,b], S. Marcellini[a], G. Masetti[a], A. Montanari[a], F.L. Navarria[a,b], A. Perrotta[a], A.M. Rossi[a,b], T. Rovelli[a,b], G.P. Siroli[a,b], N. Tosi[a,b], R. Travaglini[a,b]

INFN Sezione di Catania [a], Università di Catania [b], CSFNSM [c], Catania, Italy

G. Cappello[a], M. Chiorboli[a,b], S. Costa[a,b], F. Giordano[a,2], R. Potenza[a,b], A. Tricomi[a,b], C. Tuve[a,b]

INFN Sezione di Firenze [a], Università di Firenze [b], Firenze, Italy

G. Barbagli[a], V. Ciulli[a,b], C. Civinini[a], R. D'Alessandro[a,b], E. Focardi[a,b], S. Gonzi[a,b], V. Gori[a,b], P. Lenzi[a,b], M. Meschini[a], S. Paoletti[a], A. Puggelli, G. Sguazzoni[a], A. Tropiano[a,b], L. Viliani[a,b]

INFN Laboratori Nazionali di Frascati, Frascati, Italy

L. Benussi, S. Bianco, F. Fabbri, D. Piccolo

INFN Sezione di Genova [a], Università di Genova [b], Genova, Italy

V. Calvelli[a,b], F. Ferro[a], M. Lo Vetere[a,b], E. Robutti[a], S. Tosi[a,b]

INFN Sezione di Milano-Bicocca [a], Università di Milano-Bicocca [b], Milano, Italy

M.E. Dinardo[a,b], S. Fiorendi[a,b], S. Gennai[a,2], R. Gerosa[a,b], A. Ghezzi[a,b], P. Govoni[a,b], S. Malvezzi[a], R.A. Manzoni[a,b], B. Marzocchi[a,b,2], D. Menasce[a], L. Moroni[a], M. Paganoni[a,b], D. Pedrini[a], S. Ragazzi[a,b], N. Redaelli[a], T. Tabarelli de Fatis[a,b]

INFN Sezione di Napoli ^{a}, Università di Napoli 'Federico II' ^{b}, Napoli, Italy, Università della Basilicata ^{c}, Potenza, Italy, Università G. Marconi ^{d}, Roma, Italy

S. Buontempo^a, N. Cavallo^{a,c}, S. Di Guida^{a,d,2}, M. Esposito^{a,b}, F. Fabozzi^{a,c}, A.O.M. Iorio^{a,b}, G. Lanza^a, L. Lista^a, S. Meola^{a,d,2}, M. Merola^a, P. Paolucci^{a,2}, C. Sciacca^{a,b}, F. Thyssen

INFN Sezione di Padova ^{a}, Università di Padova ^{b}, Padova, Italy, Università di Trento ^{c}, Trento, Italy

P. Azzi^{a,2}, N. Bacchetta^a, D. Bisello^{a,b}, R. Carlin^{a,b}, A. Carvalho Antunes De Oliveira^{a,b}, P. Checchia^a, M. Dall'Osso^{a,b}, T. Dorigo^a, U. Dosselli^a, F. Gasparini^{a,b}, U. Gasparini^{a,b}, F. Gonella^a, A. Gozzelino^a, S. Lacaprara^a, M. Margoni^{a,b}, A.T. Meneguzzo^{a,b}, M. Michelotto^a, J. Pazzini^{a,b}, N. Pozzobon^{a,b}, P. Ronchese^{a,b}, F. Simonetto^{a,b}, E. Torassa^a, M. Tosi^{a,b}, M. Zanetti, P. Zotto^{a,b}, A. Zucchetta^{a,b}, G. Zumerle^{a,b}

INFN Sezione di Pavia ^{a}, Università di Pavia ^{b}, Pavia, Italy

A. Braghieri^a, M. Gabusi^{a,b}, A. Magnani^a, S.P. Ratti^{a,b}, V. Re^a, C. Riccardi^{a,b}, P. Salvini^a, I. Vai^a, P. Vitulo^{a,b}

INFN Sezione di Perugia ^{a}, Università di Perugia ^{b}, Perugia, Italy

L. Alunni Solestizi^{a,b}, M. Biasini^{a,b}, G.M. Bilei^a, D. Ciangottini^{a,b,2}, L. Fanò^{a,b}, P. Lariccia^{a,b}, G. Mantovani^{a,b}, M. Menichelli^a, A. Saha^a, A. Santocchia^{a,b}, A. Spiezia^{a,b,2}

INFN Sezione di Pisa ^{a}, Università di Pisa ^{b}, Scuola Normale Superiore di Pisa ^{c}, Pisa, Italy

K. Androsov^{a,29}, P. Azzurri^a, G. Bagliesi^a, J. Bernardini^a, T. Boccali^a, G. Broccolo^{a,c}, R. Castaldi^a, M.A. Ciocci^{a,29}, R. Dell'Orso^a, S. Donato^{a,c,2}, G. Fedi, L. Foà^{a,c†}, A. Giassi^a, M.T. Grippo^{a,29}, F. Ligabue^{a,c}, T. Lomtadze^a, L. Martini^{a,b}, A. Messineo^{a,b}, F. Palla^a, A. Rizzi^{a,b}, A. Savoy-Navarro^{a,30}, A.T. Serban^a, P. Spagnolo^a, P. Squillacioti^{a,29}, R. Tenchini^a, G. Tonelli^{a,b}, A. Venturi^a, P.G. Verdini^a

INFN Sezione di Roma ^{a}, Università di Roma ^{b}, Roma, Italy

L. Barone^{a,b}, F. Cavallari^a, G. D'imperio^{a,b}, D. Del Re^{a,b}, M. Diemoz^a, S. Gelli^{a,b}, C. Jorda^a, E. Longo^{a,b}, F. Margaroli^{a,b}, P. Meridiani^a, F. Micheli^{a,b}, G. Organtini^{a,b}, R. Paramatti^a, F. Preiato^{a,b}, S. Rahatlou^{a,b}, C. Rovelli^a, F. Santanastasio^{a,b}, L. Soffi^{a,b}, P. Traczyk^{a,b,2}

INFN Sezione di Torino ^{a}, Università di Torino ^{b}, Torino, Italy, Università del Piemonte Orientale ^{c}, Novara, Italy

N. Amapane^{a,b}, R. Arcidiacono^{a,c}, S. Argiro^{a,b}, M. Arneodo^{a,c}, R. Bellan^{a,b}, C. Biino^a, N. Cartiglia^a, S. Casasso^{a,b}, M. Costa^{a,b}, R. Covarelli^{a,b}, A. Degano^{a,b}, N. Demaria^a, L. Finco^{a,b,2}, B. Kiani^{a,b}, C. Mariotti^a, S. Maselli^a, E. Migliore^{a,b}, V. Monaco^{a,b}, M. Musich^a, M.M. Obertino^{a,c}, L. Pacher^{a,b}, N. Pastrone^a, M. Pelliccioni^a, G.L. Pinna Angioni^{a,b}, A. Romero^{a,b}, M. Ruspa^{a,c}, R. Sacchi^{a,b}, A. Solano^{a,b}, A. Staiano^a, U. Tamponi^a

INFN Sezione di Trieste [a], **Università di Trieste** [b], **Trieste, Italy**

S. Belforte[a], V. Candelise[a,b,2], M. Casarsa[a], F. Cossutti[a], G. Della Ricca[a,b], B. Gobbo[a], C. La Licata[a,b], M. Marone[a,b], A. Schizzi[a,b], T. Umer[a,b], A. Zanetti[a]

Kangwon National University, Chunchon, Korea

S. Chang, A. Kropivnitskaya, S.K. Nam

Kyungpook National University, Daegu, Korea

D.H. Kim, G.N. Kim, M.S. Kim, D.J. Kong, S. Lee, Y.D. Oh, A. Sakharov, D.C. Son

Chonbuk National University, Jeonju, Korea

H. Kim, T.J. Kim, M.S. Ryu

Chonnam National University, Institute for Universe and Elementary Particles, Kwangju, Korea

S. Song

Korea University, Seoul, Korea

S. Choi, Y. Go, D. Gyun, B. Hong, M. Jo, H. Kim, Y. Kim, B. Lee, K. Lee, K.S. Lee, S. Lee, S.K. Park, Y. Roh

Seoul National University, Seoul, Korea

H.D. Yoo

University of Seoul, Seoul, Korea

M. Choi, J.H. Kim, J.S.H. Lee, I.C. Park, G. Ryu

Sungkyunkwan University, Suwon, Korea

Y. Choi, Y.K. Choi, J. Goh, D. Kim, E. Kwon, J. Lee, I. Yu

Vilnius University, Vilnius, Lithuania

A. Juodagalvis, J. Vaitkus

National Centre for Particle Physics, Universiti Malaya, Kuala Lumpur, Malaysia

Z.A. Ibrahim, J.R. Komaragiri, M.A.B. Md Ali[31], F. Mohamad Idris, W.A.T. Wan Abdullah

Centro de Investigacion y de Estudios Avanzados del IPN, Mexico City, Mexico

E. Casimiro Linares, H. Castilla-Valdez, E. De La Cruz-Burelo, I. Heredia-de La Cruz[32], A. Hernandez-Almada, R. Lopez-Fernandez, G. Ramirez Sanchez, A. Sanchez-Hernandez

Universidad Iberoamericana, Mexico City, Mexico

S. Carrillo Moreno, F. Vazquez Valencia

Benemerita Universidad Autonoma de Puebla, Puebla, Mexico

S. Carpinteyro, I. Pedraza, H.A. Salazar Ibarguen

Universidad Autónoma de San Luis Potosí, San Luis Potosí, Mexico

A. Morelos Pineda

University of Auckland, Auckland, New Zealand

D. Krofcheck

University of Canterbury, Christchurch, New Zealand

P.H. Butler, S. Reucroft

National Centre for Physics, Quaid-I-Azam University, Islamabad, Pakistan

A. Ahmad, M. Ahmad, Q. Hassan, H.R. Hoorani, W.A. Khan, T. Khurshid, M. Shoaib

National Centre for Nuclear Research, Swierk, Poland

H. Bialkowska, M. Bluj, B. Boimska, T. Frueboes, M. Górski, M. Kazana, K. Nawrocki, K. Romanowska-Rybinska, M. Szleper, P. Zalewski

Institute of Experimental Physics, Faculty of Physics, University of Warsaw, Warsaw, Poland

G. Brona, K. Bunkowski, K. Doroba, A. Kalinowski, M. Konecki, J. Krolikowski, M. Misiura, M. Olszewski, M. Walczak

Laboratório de Instrumentação e Física Experimental de Partículas, Lisboa, Portugal

P. Bargassa, C. Beirão Da Cruz E Silva, A. Di Francesco, P. Faccioli, P.G. Ferreira Parracho, M. Gallinaro, L. Lloret Iglesias, F. Nguyen, J. Rodrigues Antunes, J. Seixas, O. Toldaiev, D. Vadruccio, J. Varela, P. Vischia

Joint Institute for Nuclear Research, Dubna, Russia

S. Afanasiev, P. Bunin, M. Gavrilenko, I. Golutvin, I. Gorbunov, A. Kamenev, V. Karjavin, V. Konoplyanikov, A. Lanev, A. Malakhov, V. Matveev[33], P. Moisenz, V. Palichik, V. Perelygin, S. Shmatov, S. Shulha, N. Skatchkov, V. Smirnov, T. Toriashvili[34], A. Zarubin

Petersburg Nuclear Physics Institute, Gatchina (St. Petersburg), Russia

V. Golovtsov, Y. Ivanov, V. Kim[35], E. Kuznetsova, P. Levchenko, V. Murzin, V. Oreshkin, I. Smirnov, V. Sulimov, L. Uvarov, S. Vavilov, A. Vorobyev

Institute for Nuclear Research, Moscow, Russia

Yu. Andreev, A. Dermenev, S. Gninenko, N. Golubev, A. Karneyeu, M. Kirsanov, N. Krasnikov, A. Pashenkov, D. Tlisov, A. Toropin

Institute for Theoretical and Experimental Physics, Moscow, Russia

V. Epshteyn, V. Gavrilov, N. Lychkovskaya, V. Popov, I. Pozdnyakov, G. Safronov, A. Spiridonov, E. Vlasov, A. Zhokin

P.N. Lebedev Physical Institute, Moscow, Russia

V. Andreev, M. Azarkin[36], I. Dremin[36], M. Kirakosyan, A. Leonidov[36], G. Mesyats, S.V. Rusakov, A. Vinogradov

Skobeltsyn Institute of Nuclear Physics, Lomonosov Moscow State University, Moscow, Russia

A. Baskakov, A. Belyaev, E. Boos, M. Dubinin[37], L. Dudko, A. Ershov, A. Gribushin, V. Klyukhin, O. Kodolova, I. Lokhtin, I. Myagkov, S. Obraztsov, S. Petrushanko, V. Savrin, A. Snigirev

State Research Center of Russian Federation, Institute for High Energy Physics, Protvino, Russia

I. Azhgirey, I. Bayshev, S. Bitioukov, V. Kachanov, A. Kalinin, D. Konstantinov, V. Krychkine, V. Petrov, R. Ryutin, A. Sobol, L. Tourtchanovitch, S. Troshin, N. Tyurin, A. Uzunian, A. Volkov

University of Belgrade, Faculty of Physics and Vinca Institute of Nuclear Sciences, Belgrade, Serbia

P. Adzic[38], M. Ekmedzic, J. Milosevic, V. Rekovic

Centro de Investigaciones Energéticas Medioambientales y Tecnológicas (CIEMAT), Madrid, Spain

J. Alcaraz Maestre, E. Calvo, M. Cerrada, M. Chamizo Llatas, N. Colino, B. De La Cruz, A. Delgado Peris, D. Domínguez Vázquez, A. Escalante Del Valle, C. Fernandez Bedoya, J.P. Fernández Ramos, J. Flix, M.C. Fouz, P. Garcia-Abia, O. Gonzalez Lopez, S. Goy Lopez, J.M. Hernandez, M.I. Josa, E. Navarro De Martino, A. Pérez-Calero Yzquierdo, J. Puerta Pelayo, A. Quintario Olmeda, I. Redondo, L. Romero, M.S. Soares

Universidad Autónoma de Madrid, Madrid, Spain

C. Albajar, J.F. de Trocóniz, M. Missiroli, D. Moran

Universidad de Oviedo, Oviedo, Spain

H. Brun, J. Cuevas, J. Fernandez Menendez, S. Folgueras, I. Gonzalez Caballero, E. Palencia Cortezon, J.M. Vizan Garcia

Instituto de Física de Cantabria (IFCA), CSIC-Universidad de Cantabria, Santander, Spain

J.A. Brochero Cifuentes, I.J. Cabrillo, A. Calderon, J.R. Castiñeiras De Saa, J. Duarte Campderros, M. Fernandez, G. Gomez, A. Graziano, A. Lopez Virto, J. Marco, R. Marco, C. Martinez Rivero, F. Matorras, F.J. Munoz Sanchez, J. Piedra Gomez, T. Rodrigo, A.Y. Rodríguez-Marrero, A. Ruiz-Jimeno, L. Scodellaro, I. Vila, R. Vilar Cortabitarte

CERN, European Organization for Nuclear Research, Geneva, Switzerland

D. Abbaneo, E. Auffray, G. Auzinger, M. Bachtis, P. Baillon, A.H. Ball, D. Barney, A. Benaglia, J. Bendavid, L. Benhabib, J.F. Benitez, G.M. Berruti, P. Bloch, A. Bocci, A. Bonato, C. Botta, H. Breuker, T. Camporesi, G. Cerminara, S. Colafranceschi[39], M. D'Alfonso, D. d'Enterria, A. Dabrowski, V. Daponte, A. David, M. De Gruttola, F. De Guio, A. De Roeck, S. De Visscher, E. Di Marco, M. Dobson, M. Dordevic, N. Dupont-Sagorin, A. Elliott-Peisert, G. Franzoni, W. Funk, D. Gigi, K. Gill, D. Giordano, M. Girone, F. Glege, R. Guida, S. Gundacker, M. Guthoff, J. Hammer, M. Hansen, P. Harris, J. Hegeman, V. Innocente, P. Janot, H. Kirschenmann, M.J. Kortelainen, K. Kousouris, K. Krajczar, P. Lecoq, C. Lourenço, M.T. Lucchini, N. Magini, L. Malgeri, M. Mannelli, J. Marrouche, A. Martelli, L. Masetti, F. Meijers, S. Mersi, E. Meschi, F. Moortgat, S. Morovic, M. Mulders, M.V. Nemallapudi, H. Neugebauer, S. Orfanelli, L. Orsini, L. Pape, E. Perez, A. Petrilli, G. Petrucciani, A. Pfeiffer, D. Piparo, A. Racz, G. Rolandi[40], M. Rovere, M. Ruan, H. Sakulin, C. Schäfer, C. Schwick, A. Sharma, P. Silva, M. Simon,

P. Sphicas[41], D. Spiga, J. Steggemann, B. Stieger, M. Stoye, Y. Takahashi, D. Treille, A. Tsirou, G.I. Veres[20], N. Wardle, H.K. Wöhri, A. Zagozdzinska[42], W.D. Zeuner

Paul Scherrer Institut, Villigen, Switzerland

W. Bertl, K. Deiters, W. Erdmann, R. Horisberger, Q. Ingram, H.C. Kaestli, D. Kotlinski, U. Langenegger, T. Rohe

Institute for Particle Physics, ETH Zurich, Zurich, Switzerland

F. Bachmair, L. Bäni, L. Bianchini, M.A. Buchmann, B. Casal, G. Dissertori, M. Dittmar, M. Donegà, M. Dünser, P. Eller, C. Grab, C. Heidegger, D. Hits, J. Hoss, G. Kasieczka, W. Lustermann, B. Mangano, A.C. Marini, M. Marionneau, P. Martinez Ruiz del Arbol, M. Masciovecchio, D. Meister, N. Mohr, P. Musella, F. Nessi-Tedaldi, F. Pandolfi, J. Pata, F. Pauss, L. Perrozzi, M. Peruzzi, M. Quittnat, M. Rossini, A. Starodumov[43], M. Takahashi, V.R. Tavolaro, K. Theofilatos, R. Wallny, H.A. Weber

Universität Zürich, Zurich, Switzerland

T.K. Aarrestad, C. Amsler[44], M.F. Canelli, V. Chiochia, A. De Cosa, C. Galloni, A. Hinzmann, T. Hreus, B. Kilminster, C. Lange, J. Ngadiuba, D. Pinna, P. Robmann, F.J. Ronga, D. Salerno, S. Taroni, Y. Yang

National Central University, Chung-Li, Taiwan

M. Cardaci, K.H. Chen, T.H. Doan, C. Ferro, M. Konyushikhin, C.M. Kuo, W. Lin, Y.J. Lu, R. Volpe, S.S. Yu

National Taiwan University (NTU), Taipei, Taiwan

P. Chang, Y.H. Chang, Y.W. Chang, Y. Chao, K.F. Chen, P.H. Chen, C. Dietz, F. Fiori, U. Grundler, W.-S. Hou, Y. Hsiung, Y.F. Liu, R.-S. Lu, M. Miñano Moya, E. Petrakou, J.f. Tsai, Y.M. Tzeng, R. Wilken

Chulalongkorn University, Faculty of Science, Department of Physics, Bangkok, Thailand

B. Asavapibhop, K. Kovitanggoon, G. Singh, N. Srimanobhas, N. Suwonjandee

Cukurova University, Adana, Turkey

A. Adiguzel, M.N. Bakirci[45], C. Dozen, I. Dumanoglu, E. Eskut, S. Girgis, G. Gokbulut, Y. Guler, E. Gurpinar, I. Hos, E.E. Kangal[46], G. Onengut[47], K. Ozdemir[48], A. Polatoz, D. Sunar Cerci[49], M. Vergili, C. Zorbilmez

Middle East Technical University, Physics Department, Ankara, Turkey

I.V. Akin, B. Bilin, S. Bilmis, B. Isildak[50], G. Karapinar[51], U.E. Surat, M. Yalvac, M. Zeyrek

Bogazici University, Istanbul, Turkey

E.A. Albayrak[52], E. Gülmez, M. Kaya[53], O. Kaya[54], T. Yetkin[55]

Istanbul Technical University, Istanbul, Turkey

K. Cankocak, Y.O. Günaydin[56], F.I. Vardarlı

Institute for Scintillation Materials of National Academy of Science of Ukraine, Kharkov, Ukraine

B. Grynyov

National Scientific Center, Kharkov Institute of Physics and Technology, Kharkov, Ukraine

L. Levchuk, P. Sorokin

University of Bristol, Bristol, United Kingdom

R. Aggleton, F. Ball, L. Beck, J.J. Brooke, E. Clement, D. Cussans, H. Flacher, J. Goldstein, M. Grimes, G.P. Heath, H.F. Heath, J. Jacob, L. Kreczko, C. Lucas, Z. Meng, D.M. Newbold[57], S. Paramesvaran, A. Poll, T. Sakuma, S. Seif El Nasr-storey, S. Senkin, D. Smith, V.J. Smith

Rutherford Appleton Laboratory, Didcot, United Kingdom

K.W. Bell, A. Belyaev[58], C. Brew, R.M. Brown, D.J.A. Cockerill, J.A. Coughlan, K. Harder, S. Harper, E. Olaiya, D. Petyt, C.H. Shepherd-Themistocleous, A. Thea, I.R. Tomalin, T. Williams, W.J. Womersley, S.D. Worm

Imperial College, London, United Kingdom

M. Baber, R. Bainbridge, O. Buchmuller, A. Bundock, D. Burton, M. Citron, D. Colling, L. Corpe, N. Cripps, P. Dauncey, G. Davies, A. De Wit, M. Della Negra, P. Dunne, A. Elwood, W. Ferguson, J. Fulcher, D. Futyan, G. Hall, G. Iles, G. Karapostoli, M. Kenzie, R. Lane, R. Lucas[57], L. Lyons, A.-M. Magnan, S. Malik, J. Nash, A. Nikitenko[43], J. Pela, M. Pesaresi, K. Petridis, D.M. Raymond, A. Richards, A. Rose, C. Seez, P. Sharp[†], A. Tapper, K. Uchida, M. Vazquez Acosta[59], T. Virdee, S.C. Zenz

Brunel University, Uxbridge, United Kingdom

J.E. Cole, P.R. Hobson, A. Khan, P. Kyberd, D. Leggat, D. Leslie, I.D. Reid, P. Symonds, L. Teodorescu, M. Turner

Baylor University, Waco, U.S.A.

A. Borzou, J. Dittmann, K. Hatakeyama, A. Kasmi, H. Liu, N. Pastika, T. Scarborough

The University of Alabama, Tuscaloosa, U.S.A.

O. Charaf, S.I. Cooper, C. Henderson, P. Rumerio

Boston University, Boston, U.S.A.

A. Avetisyan, T. Bose, C. Fantasia, D. Gastler, P. Lawson, D. Rankin, C. Richardson, J. Rohlf, J. St. John, L. Sulak, D. Zou

Brown University, Providence, U.S.A.

J. Alimena, E. Berry, S. Bhattacharya, D. Cutts, Z. Demiragli, N. Dhingra, A. Ferapontov, A. Garabedian, U. Heintz, E. Laird, G. Landsberg, Z. Mao, M. Narain, S. Sagir, T. Sinthuprasith

University of California, Davis, Davis, U.S.A.

R. Breedon, G. Breto, M. Calderon De La Barca Sanchez, S. Chauhan, M. Chertok, J. Conway, R. Conway, P.T. Cox, R. Erbacher, M. Gardner, W. Ko, R. Lander, M. Mulhearn,

D. Pellett, J. Pilot, F. Ricci-Tam, S. Shalhout, J. Smith, M. Squires, D. Stolp, M. Tripathi, S. Wilbur, R. Yohay

University of California, Los Angeles, U.S.A.

R. Cousins, P. Everaerts, C. Farrell, J. Hauser, M. Ignatenko, G. Rakness, D. Saltzberg, E. Takasugi, V. Valuev, M. Weber

University of California, Riverside, Riverside, U.S.A.

K. Burt, R. Clare, J. Ellison, J.W. Gary, G. Hanson, J. Heilman, M. Ivova Rikova, P. Jandir, E. Kennedy, F. Lacroix, O.R. Long, A. Luthra, M. Malberti, M. Olmedo Negrete, A. Shrinivas, S. Sumowidagdo, H. Wei, S. Wimpenny

University of California, San Diego, La Jolla, U.S.A.

J.G. Branson, G.B. Cerati, S. Cittolin, R.T. D'Agnolo, A. Holzner, R. Kelley, D. Klein, D. Kovalskyi, J. Letts, I. Macneill, D. Olivito, S. Padhi, M. Pieri, M. Sani, V. Sharma, S. Simon, M. Tadel, Y. Tu, A. Vartak, S. Wasserbaech[60], C. Welke, F. Würthwein, A. Yagil, G. Zevi Della Porta

University of California, Santa Barbara, Santa Barbara, U.S.A.

D. Barge, J. Bradmiller-Feld, C. Campagnari, A. Dishaw, V. Dutta, K. Flowers, M. Franco Sevilla, P. Geffert, C. George, F. Golf, L. Gouskos, J. Gran, J. Incandela, C. Justus, N. Mccoll, S.D. Mullin, J. Richman, D. Stuart, W. To, C. West, J. Yoo

California Institute of Technology, Pasadena, U.S.A.

D. Anderson, A. Apresyan, A. Bornheim, J. Bunn, Y. Chen, J. Duarte, A. Mott, H.B. Newman, C. Pena, M. Pierini, M. Spiropulu, J.R. Vlimant, S. Xie, R.Y. Zhu

Carnegie Mellon University, Pittsburgh, U.S.A.

V. Azzolini, A. Calamba, B. Carlson, T. Ferguson, Y. Iiyama, M. Paulini, J. Russ, M. Sun, H. Vogel, I. Vorobiev

University of Colorado at Boulder, Boulder, U.S.A.

J.P. Cumalat, W.T. Ford, A. Gaz, F. Jensen, A. Johnson, M. Krohn, T. Mulholland, U. Nauenberg, J.G. Smith, K. Stenson, S.R. Wagner

Cornell University, Ithaca, U.S.A.

J. Alexander, A. Chatterjee, J. Chaves, J. Chu, S. Dittmer, N. Eggert, N. Mirman, G. Nicolas Kaufman, J.R. Patterson, A. Rinkevicius, A. Ryd, L. Skinnari, W. Sun, S.M. Tan, W.D. Teo, J. Thom, J. Thompson, J. Tucker, Y. Weng, P. Wittich

Fermi National Accelerator Laboratory, Batavia, U.S.A.

S. Abdullin, M. Albrow, J. Anderson, G. Apollinari, L.A.T. Bauerdick, A. Beretvas, J. Berryhill, P.C. Bhat, G. Bolla, K. Burkett, J.N. Butler, H.W.K. Cheung, F. Chlebana, S. Cihangir, V.D. Elvira, I. Fisk, J. Freeman, E. Gottschalk, L. Gray, D. Green, S. Grünendahl, O. Gutsche, J. Hanlon, D. Hare, R.M. Harris, J. Hirschauer, B. Hooberman, Z. Hu, S. Jindariani, M. Johnson, U. Joshi, A.W. Jung, B. Klima, B. Kreis, S. Kwan[†], S. Lammel, J. Linacre, D. Lincoln, R. Lipton, T. Liu, R. Lopes De Sá, J. Lykken, K. Maeshima, J.M. Marraffino, V.I. Martinez Outschoorn, S. Maruyama,

D. Mason, P. McBride, P. Merkel, K. Mishra, S. Mrenna, S. Nahn, C. Newman-Holmes, V. O'Dell, O. Prokofyev, E. Sexton-Kennedy, A. Soha, W.J. Spalding, L. Spiegel, L. Taylor, S. Tkaczyk, N.V. Tran, L. Uplegger, E.W. Vaandering, C. Vernieri, M. Verzocchi, R. Vidal, A. Whitbeck, F. Yang, H. Yin

University of Florida, Gainesville, U.S.A.

D. Acosta, P. Avery, P. Bortignon, D. Bourilkov, A. Carnes, M. Carver, D. Curry, S. Das, G.P. Di Giovanni, R.D. Field, M. Fisher, I.K. Furic, J. Hugon, J. Konigsberg, A. Korytov, T. Kypreos, J.F. Low, P. Ma, K. Matchev, H. Mei, P. Milenovic[61], G. Mitselmakher, L. Muniz, D. Rank, L. Shchutska, M. Snowball, D. Sperka, S.J. Wang, J. Yelton

Florida International University, Miami, U.S.A.

S. Hewamanage, S. Linn, P. Markowitz, G. Martinez, J.L. Rodriguez

Florida State University, Tallahassee, U.S.A.

A. Ackert, J.R. Adams, T. Adams, A. Askew, J. Bochenek, B. Diamond, J. Haas, S. Hagopian, V. Hagopian, K.F. Johnson, A. Khatiwada, H. Prosper, V. Veeraraghavan, M. Weinberg

Florida Institute of Technology, Melbourne, U.S.A.

V. Bhopatkar, M. Hohlmann, H. Kalakhety, D. Mareskas-palcek, T. Roy, F. Yumiceva

University of Illinois at Chicago (UIC), Chicago, U.S.A.

M.R. Adams, L. Apanasevich, D. Berry, R.R. Betts, I. Bucinskaite, R. Cavanaugh, O. Evdokimov, L. Gauthier, C.E. Gerber, D.J. Hofman, P. Kurt, C. O'Brien, I.D. Sandoval Gonzalez, C. Silkworth, P. Turner, N. Varelas, Z. Wu, M. Zakaria

The University of Iowa, Iowa City, U.S.A.

B. Bilki[62], W. Clarida, K. Dilsiz, S. Durgut, R.P. Gandrajula, M. Haytmyradov, V. Khristenko, J.-P. Merlo, H. Mermerkaya[63], A. Mestvirishvili, A. Moeller, J. Nachtman, H. Ogul, Y. Onel, F. Ozok[52], A. Penzo, S. Sen, C. Snyder, P. Tan, E. Tiras, J. Wetzel, K. Yi

Johns Hopkins University, Baltimore, U.S.A.

I. Anderson, B.A. Barnett, B. Blumenfeld, S. Bolognesi, D. Fehling, L. Feng, A.V. Gritsan, P. Maksimovic, C. Martin, K. Nash, M. Osherson, M. Swartz, M. Xiao, Y. Xin

The University of Kansas, Lawrence, U.S.A.

P. Baringer, A. Bean, G. Benelli, C. Bruner, J. Gray, R.P. Kenny III, D. Majumder, M. Malek, M. Murray, D. Noonan, S. Sanders, R. Stringer, Q. Wang, J.S. Wood

Kansas State University, Manhattan, U.S.A.

I. Chakaberia, A. Ivanov, K. Kaadze, S. Khalil, M. Makouski, Y. Maravin, L.K. Saini, N. Skhirtladze, I. Svintradze

Lawrence Livermore National Laboratory, Livermore, U.S.A.

D. Lange, F. Rebassoo, D. Wright

University of Maryland, College Park, U.S.A.

C. Anelli, A. Baden, O. Baron, A. Belloni, B. Calvert, S.C. Eno, C. Ferraioli, J.A. Gomez, N.J. Hadley, S. Jabeen, R.G. Kellogg, T. Kolberg, J. Kunkle, Y. Lu, A.C. Mignerey, K. Pedro, Y.H. Shin, A. Skuja, M.B. Tonjes, S.C. Tonwar

Massachusetts Institute of Technology, Cambridge, U.S.A.

A. Apyan, R. Barbieri, A. Baty, K. Bierwagen, S. Brandt, W. Busza, I.A. Cali, L. Di Matteo, G. Gomez Ceballos, M. Goncharov, D. Gulhan, M. Klute, Y.S. Lai, Y.-J. Lee, A. Levin, P.D. Luckey, C. Mcginn, X. Niu, C. Paus, D. Ralph, C. Roland, G. Roland, G.S.F. Stephans, K. Sumorok, M. Varma, D. Velicanu, J. Veverka, J. Wang, T.W. Wang, B. Wyslouch, M. Yang, V. Zhukova

University of Minnesota, Minneapolis, U.S.A.

B. Dahmes, A. Finkel, A. Gude, S.C. Kao, K. Klapoetke, Y. Kubota, J. Mans, S. Nourbakhsh, R. Rusack, N. Tambe, J. Turkewitz

University of Mississippi, Oxford, U.S.A.

J.G. Acosta, S. Oliveros

University of Nebraska-Lincoln, Lincoln, U.S.A.

E. Avdeeva, K. Bloom, S. Bose, D.R. Claes, A. Dominguez, C. Fangmeier, R. Gonzalez Suarez, R. Kamalieddin, J. Keller, D. Knowlton, I. Kravchenko, J. Lazo-Flores, F. Meier, J. Monroy, F. Ratnikov, J.E. Siado, G.R. Snow

State University of New York at Buffalo, Buffalo, U.S.A.

M. Alyari, J. Dolen, J. George, A. Godshalk, I. Iashvili, J. Kaisen, A. Kharchilava, A. Kumar, S. Rappoccio

Northeastern University, Boston, U.S.A.

G. Alverson, E. Barberis, D. Baumgartel, M. Chasco, A. Hortiangtham, A. Massironi, D.M. Morse, D. Nash, T. Orimoto, R. Teixeira De Lima, D. Trocino, R.-J. Wang, D. Wood, J. Zhang

Northwestern University, Evanston, U.S.A.

K.A. Hahn, A. Kubik, N. Mucia, N. Odell, B. Pollack, A. Pozdnyakov, M. Schmitt, S. Stoynev, K. Sung, M. Trovato, M. Velasco, S. Won

University of Notre Dame, Notre Dame, U.S.A.

A. Brinkerhoff, N. Dev, M. Hildreth, C. Jessop, D.J. Karmgard, N. Kellams, K. Lannon, S. Lynch, N. Marinelli, F. Meng, C. Mueller, Y. Musienko[33], T. Pearson, M. Planer, R. Ruchti, G. Smith, N. Valls, M. Wayne, M. Wolf, A. Woodard

The Ohio State University, Columbus, U.S.A.

L. Antonelli, J. Brinson, B. Bylsma, L.S. Durkin, S. Flowers, A. Hart, C. Hill, R. Hughes, K. Kotov, T.Y. Ling, B. Liu, W. Luo, D. Puigh, M. Rodenburg, B.L. Winer, H.W. Wulsin

Princeton University, Princeton, U.S.A.

O. Driga, P. Elmer, J. Hardenbrook, P. Hebda, S.A. Koay, P. Lujan, D. Marlow, T. Medvedeva, M. Mooney, J. Olsen, C. Palmer, P. Piroué, X. Quan, H. Saka, D. Stickland, C. Tully, J.S. Werner, A. Zuranski

Purdue University, West Lafayette, U.S.A.

V.E. Barnes, D. Benedetti, D. Bortoletto, L. Gutay, M.K. Jha, M. Jones, K. Jung, M. Kress, N. Leonardo, D.H. Miller, N. Neumeister, F. Primavera, B.C. Radburn-Smith, X. Shi, I. Shipsey, D. Silvers, J. Sun, A. Svyatkovskiy, F. Wang, W. Xie, L. Xu, J. Zablocki

Purdue University Calumet, Hammond, U.S.A.

N. Parashar, J. Stupak

Rice University, Houston, U.S.A.

A. Adair, B. Akgun, Z. Chen, K.M. Ecklund, F.J.M. Geurts, M. Guilbaud, W. Li, B. Michlin, M. Northup, B.P. Padley, R. Redjimi, J. Roberts, J. Rorie, Z. Tu, J. Zabel

University of Rochester, Rochester, U.S.A.

B. Betchart, A. Bodek, P. de Barbaro, R. Demina, Y. Eshaq, T. Ferbel, M. Galanti, A. Garcia-Bellido, P. Goldenzweig, J. Han, A. Harel, O. Hindrichs, A. Khukhunaishvili, G. Petrillo, M. Verzetti, D. Vishnevskiy

The Rockefeller University, New York, U.S.A.

L. Demortier

Rutgers, The State University of New Jersey, Piscataway, U.S.A.

S. Arora, A. Barker, J.P. Chou, C. Contreras-Campana, E. Contreras-Campana, D. Duggan, D. Ferencek, Y. Gershtein, R. Gray, E. Halkiadakis, D. Hidas, E. Hughes, S. Kaplan, R. Kunnawalkam Elayavalli, A. Lath, S. Panwalkar, M. Park, S. Salur, S. Schnetzer, D. Sheffield, S. Somalwar, R. Stone, S. Thomas, P. Thomassen, M. Walker

University of Tennessee, Knoxville, U.S.A.

M. Foerster, G. Riley, K. Rose, S. Spanier, A. York

Texas A&M University, College Station, U.S.A.

O. Bouhali[64], A. Castaneda Hernandez, M. Dalchenko, M. De Mattia, A. Delgado, S. Dildick, R. Eusebi, W. Flanagan, J. Gilmore, T. Kamon[65], V. Krutelyov, R. Montalvo, R. Mueller, I. Osipenkov, Y. Pakhotin, R. Patel, A. Perloff, J. Roe, A. Rose, A. Safonov, I. Suarez, A. Tatarinov, K.A. Ulmer

Texas Tech University, Lubbock, U.S.A.

N. Akchurin, C. Cowden, J. Damgov, C. Dragoiu, P.R. Dudero, J. Faulkner, S. Kunori, K. Lamichhane, S.W. Lee, T. Libeiro, S. Undleeb, I. Volobouev

Vanderbilt University, Nashville, U.S.A.

E. Appelt, A.G. Delannoy, S. Greene, A. Gurrola, R. Janjam, W. Johns, C. Maguire, Y. Mao, A. Melo, P. Sheldon, B. Snook, S. Tuo, J. Velkovska, Q. Xu

University of Virginia, Charlottesville, U.S.A.

M.W. Arenton, S. Boutle, B. Cox, B. Francis, J. Goodell, R. Hirosky, A. Ledovskoy, H. Li, C. Lin, C. Neu, E. Wolfe, J. Wood, F. Xia

Wayne State University, Detroit, U.S.A.

C. Clarke, R. Harr, P.E. Karchin, C. Kottachchi Kankanamge Don, P. Lamichhane, J. Sturdy

University of Wisconsin, Madison, U.S.A.

D.A. Belknap, D. Carlsmith, M. Cepeda, A. Christian, S. Dasu, L. Dodd, S. Duric, E. Friis, B. Gomber, R. Hall-Wilton, M. Herndon, A. Hervé, P. Klabbers, A. Lanaro, A. Levine, K. Long, R. Loveless, A. Mohapatra, I. Ojalvo, T. Perry, G.A. Pierro, G. Polese, I. Ross, T. Ruggles, T. Sarangi, A. Savin, N. Smith, W.H. Smith, D. Taylor, N. Woods

†: Deceased
1: Also at Vienna University of Technology, Vienna, Austria
2: Also at CERN, European Organization for Nuclear Research, Geneva, Switzerland
3: Also at State Key Laboratory of Nuclear Physics and Technology, Peking University, Beijing, China
4: Also at Institut Pluridisciplinaire Hubert Curien, Université de Strasbourg, Université de Haute Alsace Mulhouse, CNRS/IN2P3, Strasbourg, France
5: Also at National Institute of Chemical Physics and Biophysics, Tallinn, Estonia
6: Also at Skobeltsyn Institute of Nuclear Physics, Lomonosov Moscow State University, Moscow, Russia
7: Also at Universidade Estadual de Campinas, Campinas, Brazil
8: Also at Centre National de la Recherche Scientifique (CNRS) - IN2P3, Paris, France
9: Also at Laboratoire Leprince-Ringuet, Ecole Polytechnique, IN2P3-CNRS, Palaiseau, France
10: Also at Joint Institute for Nuclear Research, Dubna, Russia
11: Also at Ain Shams University, Cairo, Egypt
12: Now at British University in Egypt, Cairo, Egypt
13: Now at Helwan University, Cairo, Egypt
14: Now at Suez University, Suez, Egypt
15: Now at Cairo University, Cairo, Egypt
16: Now at Fayoum University, El-Fayoum, Egypt
17: Also at Université de Haute Alsace, Mulhouse, France
18: Also at Brandenburg University of Technology, Cottbus, Germany
19: Also at Institute of Nuclear Research ATOMKI, Debrecen, Hungary
20: Also at Eötvös Loránd University, Budapest, Hungary
21: Also at University of Debrecen, Debrecen, Hungary
22: Also at Wigner Research Centre for Physics, Budapest, Hungary
23: Also at University of Visva-Bharati, Santiniketan, India
24: Now at King Abdulaziz University, Jeddah, Saudi Arabia
25: Also at University of Ruhuna, Matara, Sri Lanka
26: Also at Isfahan University of Technology, Isfahan, Iran
27: Also at University of Tehran, Department of Engineering Science, Tehran, Iran
28: Also at Plasma Physics Research Center, Science and Research Branch, Islamic Azad University, Tehran, Iran

29: Also at Università degli Studi di Siena, Siena, Italy

30: Also at Purdue University, West Lafayette, U.S.A.

31: Also at International Islamic University of Malaysia, Kuala Lumpur, Malaysia

32: Also at CONSEJO NATIONAL DE CIENCIA Y TECNOLOGIA, MEXICO, Mexico

33: Also at Institute for Nuclear Research, Moscow, Russia

34: Also at Institute of High Energy Physics and Informatization, Tbilisi State University, Tbilisi, Georgia

35: Also at St. Petersburg State Polytechnical University, St. Petersburg, Russia

36: Also at National Research Nuclear University 'Moscow Engineering Physics Institute' (MEPhI), Moscow, Russia

37: Also at California Institute of Technology, Pasadena, U.S.A.

38: Also at Faculty of Physics, University of Belgrade, Belgrade, Serbia

39: Also at Facoltà Ingegneria, Università di Roma, Roma, Italy

40: Also at Scuola Normale e Sezione dell'INFN, Pisa, Italy

41: Also at University of Athens, Athens, Greece

42: Also at Warsaw University of Technology, Institute of Electronic Systems, Warsaw, Poland

43: Also at Institute for Theoretical and Experimental Physics, Moscow, Russia

44: Also at Albert Einstein Center for Fundamental Physics, Bern, Switzerland

45: Also at Gaziosmanpasa University, Tokat, Turkey

46: Also at Mersin University, Mersin, Turkey

47: Also at Cag University, Mersin, Turkey

48: Also at Piri Reis University, Istanbul, Turkey

49: Also at Adiyaman University, Adiyaman, Turkey

50: Also at Ozyegin University, Istanbul, Turkey

51: Also at Izmir Institute of Technology, Izmir, Turkey

52: Also at Mimar Sinan University, Istanbul, Istanbul, Turkey

53: Also at Marmara University, Istanbul, Turkey

54: Also at Kafkas University, Kars, Turkey

55: Also at Yildiz Technical University, Istanbul, Turkey

56: Also at Kahramanmaras Sütcü Imam University, Kahramanmaras, Turkey

57: Also at Rutherford Appleton Laboratory, Didcot, United Kingdom

58: Also at School of Physics and Astronomy, University of Southampton, Southampton, United Kingdom

59: Also at Instituto de Astrofísica de Canarias, La Laguna, Spain

60: Also at Utah Valley University, Orem, U.S.A.

61: Also at University of Belgrade, Faculty of Physics and Vinca Institute of Nuclear Sciences, Belgrade, Serbia

62: Also at Argonne National Laboratory, Argonne, U.S.A.

63: Also at Erzincan University, Erzincan, Turkey

64: Also at Texas A&M University at Qatar, Doha, Qatar

65: Also at Kyungpook National University, Daegu, Korea